REPUBLIC OF TÜRKİYE
HARRAN UNIVERSITY
INSTITUTE OF GRADUATE EDUCATION

MASTER THESIS

PRODUCTION OF CUO AND CU COMPLEX DOPED ZNO FILMS, INVESTIGATION OF THEIR STRUCTURAL, OPTICAL AND RADIATION SHIELDING BEHAVIORS

KOCHAR SALIH ARIF ARIF

BIOMATERIALS AND TISSUE ENGINEERING

Şanlıurfa
2025

REPUBLIC OF TÜRKİYE
HARRAN UNIVERSITY

MASTER THESIS

PRODUCTION OF CUO AND CU COMPLEX DOPED ZNO FILMS, INVESTIGATION OF THEIR STRUCTURAL, OPTICAL AND RADIATION SHIELDING BEHAVIORS

KOCHAR SALIH ARIF ARIF

BIOMATERIALS AND TISSUE ENGINEERING
Thesis Supervisor: Prof. Dr. ŞERİFE YALÇIN

Şanlıurfa
2025

ACKNOWLEDGEMENT

First and foremost, I would like to express my deepest gratitude to Allah for granting me the strength, patience, and perseverance required to successfully complete my master's studies and this thesis.

I am sincerely thankful to my advisor, **Prof. Dr. Şerife Yalçın** of the Harran University Department of Physics, for her invaluable guidance, encouragement, and continuous support. From the selection of the research topic to the final stages of writing, her knowledge, expertise, and mentorship have been essential to the successful completion of this work.

My gratitude is further extended to the **HÜBAP (25068)** for providing the financial support necessary to carry out this study.

I am deeply indebted to my colleagues and friends, especially **Engineer Ahmed**, for their encouragement, insightful discussions, and valuable support, all of which enriched my research experience.

Above all, I owe my profound gratitude to my beloved family for their unwavering love, prayers, and encouragement. In particular, my mother and elder sister have been a constant source of strength and motivation.

Finally, I would like to thank the members of my examination committee for their constructive feedback and thoughtful evaluation of my thesis.

İÇİNDEKİLER

ABSTRACT

MASTER THESIS

PRODUCTION OF CUO AND CU COMPLEX DOPED ZNO FILMS, INVESTIGATION OF THEIR STRUCTURAL, OPTICAL AND RADIATION SHIELDING BEHAVIORS

KOCHAR SALIH ARIF ARIF

HARRAN UNIVERSITY
INSTITUTE OF GRADUATE EDUCATION
BIOMATERIALS AND TISSUE ENGINEERING

Thesis Supervisor: Prof. Dr. ŞERİFE YALÇIN
Year:2025, Page : 53

Structural, optical, and radiation response features of copper zinc oxide CuZnO thin films made by sol-gel spin coating are listed here. ZnO, Cu doped ZnO 1,3 and 5 wt , and Cu complex doped ZnO 1,3 and 5 wt were seven thin films created and then put through gamma radiation to test their abilities under different conditions. Research was about how Cu and complex addition changed ZnO thin films characteristics. X-ray diffraction XRD analysis showed notable changes in size, strain, and crystalline Cu and complex added samples as expected with better textured grains and more uniform structure.UV-Vis light detected a decrease in the ZnO film bandgap when Cu and Cu complex were added, increasing how much visible light could be taken in. Raman spectroscopy studied vibrational modes before and after irradiation; the peaks of all the peaks were seen to broaden and shift broadly, especially in the doped samples, as consistent with changing phonon coupling and defect structure. Moreover, radiation exposure caused highly minute changes in peak position and loss of intensity, testifying to the gamma-radiation sensitivity of the films.Results position CuZnO thin films at the forefront as next-generation material for optoelectronic devices, radiation sensors, and environmental monitoring systems.The current work contributes to metal-oxide semiconductor literature and aims to prove the importance of formulating low-cost and environmentally friendly synthesis processes for the application of high end materials.

KEYWORDS: SEM, ZnO, Radiation shielding, Raman spectroscopy, Spin coating, CuO

ABSTRACT

YÜKSEK LİSANS TEZİ

CUO VE CU KOMPLEKSİ KATKILI ZNO FİLMLERİN ÜRETİLMESİ, YAPISAL, OPTİK VE RADYASYON ZIRHLAMA DAVRANIŞLARININ ARAŞTIRILMASI

KOCHAR SALIH ARIF ARIF

HARRAN ÜNİVERSİTESİ
LİSANSÜSTÜ EĞİTİM ENSTİTÜSÜ
BİYOMALZEME VE DOKU MÜHENDİSLİĞİ

Tez Danışmanı:Prof. Dr. ŞERİFE YALÇIN
Yıl:2025, Sayfa : 53

Bu tez çalışmasında, sol-jel spin kaplama yöntemi kullanılarak bakır katkılı çinko oksit (CuZnO)(%1,3 ve %5 ağırlık) ve bakır kompleksi katkılı ZnO filmler (%1,3 ve %5 ağırlık) üretilmiş ve üretilen filmlerinin yapısal, optik ve radyasyon tepki özellikleri araştırılmıştır. Araştırma, bakır ve kompleks ilavesinin ZnO ince filmlerinin fizikokimyasal özellikleri üzerindeki etkisine odaklanmıştır. X-ışını kırınımı (XRD) analizi, bakır ve kompleks ilavesiyle kristalit boyutunda, kafes gerginliğinde ve kristalinitede önemli farklılıklar olduğunu göstermiştir; bu, tane dokusu ve yapısal homojenliğin iyileştirilmesiyle beklenebilir. UV-Vis spektroskopisi, Cu ve Cu kompleks ilavesiyle ZnO filminin optik bant aralığındaki azalmayı ve görünür ışık emiliminin arttığını ortaya koymuştur. Raman spektroskopisi, Tüm piklerin, özellikle katkılı numunelerde, değişen fonon kuplajı ve kusur yapısıyla tutarlı olarak genişlediği ve geniş ölçüde kaydığı görülmüştür. Sonuçlar, CuZnO ince filmlerini optoelektronik cihazlar, radyasyon sensörleri ve çevresel izleme sistemleri için yeni nesil malzeme olarak ön plana çıkarmaktadır. Bu çalışma, metal oksit yarı iletken literatürüne katkıda bulunmakta ve yüksek kaliteli malzemelerin uygulanması için düşük maliyetli ve çevre dostu sentez süreçlerinin formüle edilmesinin önemini kanıtlamayı amaçlamaktadır. Tıbbi fizik alanında, bu tür radyasyona duyarlı ince filmler, radyoterapi ve tanısal görüntüleme sırasında hasta ve personel maruziyetinin izlenmesi için gelişmiş dozimetreler ve sensörler geliştirmede uygulama alanı bulabilir.

ANAHTAR KELİMELER: SEM, ZnO, Radyasyon koruması, Raman spektroskopisi, Spin kaplama, CuO

ŞEKİLLER DİZİNİ

ÇİZELGELER DİZİNİ

SYMBOLS

Mililitre	mL
ρ	resistivity
Å	Angstrom
Bq	Becquerel
Eg	Bandgap
keV	kilo electron volt
keV	kilo electron volt
°C	Temperature
λ	Dalga Boyu
µL	Microliter
ρ	density (kg/m3)

ABBREVIATIONS

CuO	Copper oxide
CVD	Chemical Vapour Deposition
CZO	Cupper Zinc Oxide
eV	Electron volt
meV	mili electron volt
PL	Photo Luminescence
PLD	pulsed laser deposition
PVD	Physical Vapour Deposition
SEM	Scanning electron microscopy
um	micrometers
uv	ultraviyole
UV-Vis	Ultraviolet Vissible
XRD	X-ray diffraction analysis
ZnO	Zinc oxide

1. INTRODUCTION

Zinc oxide (ZnO) is a highly useful and well-researched material with a staggering number of applications in all areas of science and technology, e.g., chemistry, materials science, biology, and nanotechnology. Its appeal lies in a combination of superior physical and chemical qualities (Ohring et all., 2002), such as wide bandgap (3.37 eV), high exciton binding energy (60 meV), and excellent optical and piezoelectric qualities. Among the advantages of ZnO is that it can be synthesized with ease and even in an environmentally friendly manner that may be achieved using a wide range of low-cost methods like sol-gel, hydrothermal, and green synthesis pathways using plant extracts. Besides ease of synthesis (Chander et all., 2022). Copper oxide (CuO and Cu_2O) is a collection of inorganic oxides of oxygen and copper. The oxides are usually found in two states: cuprous oxide (Cu_2O) when copper is in the +1 oxidation state and cupric oxide (CuO) when copper is in the +2 oxidation state. Copper oxides are particularly of interest due to their diverse uses in catalysis, semiconductors (Amani et all., 2024), sensors, antimicrobial compounds and other chemical and industrial uses. The properties of ZnO and CuO materials are given in Table 1.1.

Table 1.1. Properties of Copper and ZnO

Property	ZnO	CuO / Cu_2O	References
Crystal Structure	Wurtzite	CuO: Monoclinic / Cu_2O: Cubic	Nazari, Moshfegh & Gholami (2013)
Bandgap Energy (eV)	3.37	CuO: ~1.2 – 1.9 / Cu_2O: ~2.0	Ghanbari, Faghihian & Zeynizadeh (2017)
Exciton Binding Energy (meV)	60	Low	Nazari, Moshfegh & Gholami (2013)
Optical Properties	UV absorption, photoluminescence	Visible region absorption	Mello, Ferreira & Souza (2013)
Biocompatibility	High	Moderate	Faghihian & Zeynizadeh (2017)
Electrical Conductivity	Semiconductor	Semiconductor	Pereira, Silva & Santos (2016)
Thermal Stability	High	Moderate	Costa, Costa & Silva (2014)

ZnO is very biocompatible and thus utilized in biomedical applications such

as drug delivery, bioimaging, antibacterial coatings, and tissue engineering. Its thermal and chemical resistance also make it a reliable component in photocatalysts, UV stabilizers, sensors, and electronic devices. In addition, when ZnO is prepared at the nanoscale level, its high reactivity and huge surface area confirm their utilities, predominantly in catalysis and air pollution remediation. All such traits make it more desirable in technology usage and basic research. (Licurgo et all., 2018),

Table 1.2. The application area, functional role of ZnO and benefits of CuO doping in CuZnO films

Property	ZnO	CuO / Cu_2O	References
Crystal Structure	Wurtzite	CuO: Monoclinic / Cu_2O: Cubic	Nazari, Moshfegh & Gholami (2013)
Bandgap Energy (eV)	3.37	CuO: ~1.2 – 1.9 / Cu_2O: ~2.0	Ghanbari, Faghihian & Zeynizadeh (2017)
Exciton Binding Energy (meV)	60	Low	Nazari, Moshfegh & Gholami (2013)
Optical Properties	UV absorption, photoluminescence	Visible region absorption	Mello, Ferreira & Souza (2013)
Biocompatibility	High	Moderate	Faghihian & Zeynizadeh (2017)
Electrical Conductivity	Semiconductor	Semiconductor	Pereira, Silva & Santos (2016)
Thermal Stability	High	Moderate	Costa, Costa & Silva (2014)

The combination of copper and zinc into a single oxide matrix may mass produce the material properties and render them very versatile to be used in many areas of diverse various technologies. CuZnO thin films using the sol-gel spin coating method provide a convenient route to deposit high-quality thin films with potential to be engineered to specification (Chen et all., 2011). For CuZnO films, sol-gel spin

coating provides the advantage of the possibility to add copper and zinc simultaneously in the oxide matrix, and this can be controlled to create the desired material properties in manufacturing to target applications (Ohring et all 2002). Further research on CuZnO thin films spans the comprehensive range of important subjects: structural properties, optical properties, and radiation sensitivity. Acquaintance with these properties is significant to foster the potential of CuZnO

thin films for best applications in best uses, primarily in optoelectronic devices such as LEDs, solar cells, and photo detectors and sensing and monitoring environmental radiation (Du et all., 2022).

1.1. What is a Thin Film?

Thin films are extremely thin layers of material, typically a few nanometers (nm) to a few micrometers (μm) thick, that are deposited on a substrate or surface. Thin films have diverse applications in science and technology because they possess distinct physical, chemical, optical, and electric characteristics, which are typically quite distinct from the characteristics of bulk material (Amani et all., 2024).

Cu:ZnO thin films have been studied in detail because they are multi-functional to be used in a range of advanced technologies. Cu:ZnO is used on solar cells, where greater optical and electronic characteristics of Cu:ZnO improve carrier transport and light absorption. Cu:ZnO films in sensors, i.e., in chemical and gas sensors, are highly sensitive and selective according to surface reactivity and selectable conductivity. In optical coating materials, for instance, anti-reflection coatings (Demircan et all., 2023), Cu doping is coupled with efficient transmission and reduced reflection of light. The films are also seen in electronic devices like transistors and other semiconductors because of their band gap energy-tunable and transparency that allows proper functioning. In addition to that, their antibacterial properties and biocompatibility make them suitable for use in biomedical devices in such a way that they are coated to provide effective as well as safe interfaces for therapeutic or diagnostic processes (Joshi et all., 2022).

1.2. Thin Film Preparation Techniques

Thin film deposition methods have a central function in the production of advanced materials used in a wide holistic array of electronic, optical, and energy devices. The methods are often categorized into two main categories: physical and chemical processes.

Sputtering is done by bombarding a target material with high-energy ions (e.g., argon ions) within a vacuum chamber. The ions collide, and atoms from the target material are expelled and deposited in a thin layer on a nearby substrate. The process is typically applied to materials with semiconductor and dielectric film.

In this procedure, the substance intended for deposition is transformed into

vapor by applying heat. The vapor then moves toward the substrate and solidifies into a slender layer. This method is commonly employed for depositing metals such as aluminum or gold, as they have relatively low vaporization temperatures (Ohring et all., 2002).

1.2.1. Physical Methods

A common thin film deposition method known as Physical Vapor Deposition (PVD) uses the vaporization of a material and then condensation onto a substrate. It is carried out under vacuum because it must stay clean. The most fundamental forms of PVD are evaporation and sputtering.

During evaporation process, heat is used to vaporize the material to be deposited. The vapor reaches the substrate and forms into a thin film. Metals like aluminum or gold are often deposited using this method since their vaporization temperatures are rather low (Mattox et all., 2010).

Sputtering involves striking a target material with high-energy ions—such as argon ions—in a vacuum chamber. The ions strike the target material, which causes atoms from that material to be ejected and deposited in a thin layer on a substrate nearby. Usually, materials having dielectric film and semiconductor are treated with this method.

During this process, the material to be deposited is vaporized using heat. The vapor travels to the substrate and condenses into a thin film. This is widely used to deposit metals like aluminum or gold since they have relatively low vaporization temperatures (Mattox et all., 2010).

1.2.2. Chemical Methods

Chemical Vapour Deposition (CVD) is another popular thin film deposition method in which reactions in the vapour phase occur to deposit a solid film on the

substrate surface. Substrates are subjected to gaseous precursors in CVD, which chemically react at high temperature to form solid films. CVD can deposit highly pure and uniform films, hence is an ideal method for semiconductor fabrication (Du et all., 2022).

Spray pyrolysis is yet another chemical technique that encompasses

atomization and spraying of a solution containing metal precursors on to a substrate in the presence of heat. On falling on the hot substrate, the solution decomposes upon heating to give a thin solid film. The process is the advantage of obtaining good-quality films at relatively low temperatures and is used widely in the production of semiconductor materials.

Substrate is dipped into a solution containing film material, is withdrawn, and an overage amount is peeled off. Annealing or drying of film is done. Such a technique is best applicable for coating substrates evenly to the huge sizes.

Sol-Gel processing is a broad process wherein a chemical solution (sol) is used to create a gel, and the gel is then deposited onto a substrate to form thin films. Sol is converted to a gel phase under certain chemical reactions, and film is heat treated or annealed after deposition to convert the gel into a solid dense thin film. It is extensively used in coating, ceramic, and optical materials applications.

Spin coating as well as dip coating are those processes in which thin film deposition is done by depositing liquid solution on the substrate. This method uses a rotating stage in which the substrate is placed on top of it, and a liquid solution is dropped onto the surface. The rotation spreads the solution evenly, and the film is annealed or dried to form a thin layer. Spin coating is commonly used in microelectronics in organic or photoresist film deposition (Bai et all., 2015); (Buzok et all., 2025); (Demircan et all., 2020).

All these chemical and physical thin film deposition technologies, among the rest, possess some advantages and applications depending on the involved materials, target properties of desired films, as well as manufacturing scale. Copper Oxide (CuO) and Zinc Oxide (ZnO) – Properties Copper Oxide (CuO) is a p-type semiconductor with a band gap ranging approximately from 1.2 to 1.9 eV. It is known for its good electrical conductivity, strong absorption in the visible spectrum, low cost, and non-toxic nature. All these properties make CuO a material of interest to be utilized in a wide range of applications including solar cells, gas sensors, antimicrobial coatings, batteries, and supercapacitors. Zinc Oxide (ZnO) is an n-type semiconductor with a wider band gap of about 3.37 eV (Amani et all., 2024). ZnO has high optical transparence, high ultraviolet (UV) absorption, and general piezoelectric and pyroelectric characteristics (Buzok et all., 2025). It is also chemically inert and biocompatible, and hence more versatile. ZnO is utilized in most UV detectors, light-emitting diodes (LEDs), gas sensors, biosensors,

photocatalysts, and cosmetic products such as sunscreens (Devi et all., 2022).

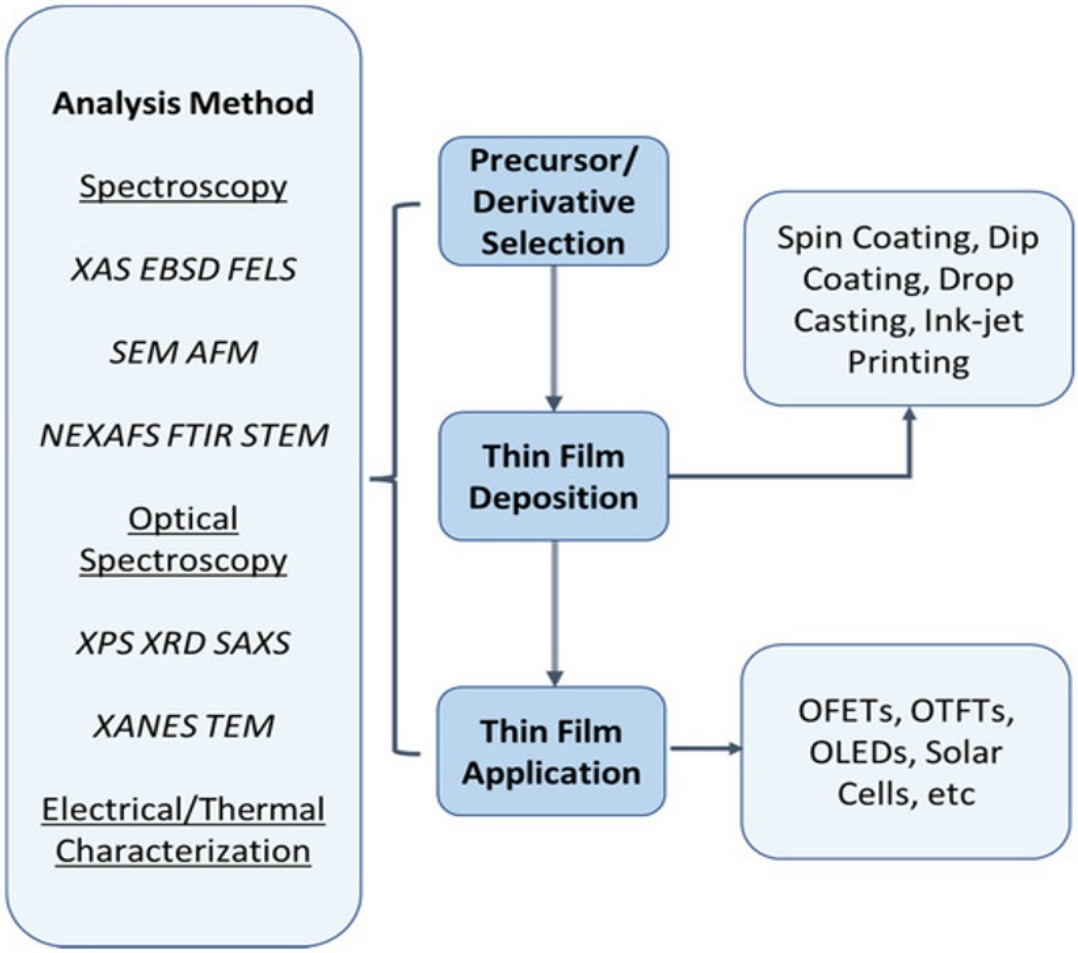

Figure 1.1. Review of the Common Deposition Methods of Thin-Film Pentacene (Fernandes, Soares & Lima, 2015)

1.3. Radiation.

Radiation shielding materials have great importance and are crucial in various fields including nuclear physics, engineering and medical applications and the need for effective shielding materials has grown significantly due to the potential hazards of ionizing radiation (Yalcin et all., 2019)

X-ray, gamma, and particle radiation are potent forms of ionizing radiation, and for their use in thin film technologies, have immense potential for new and unique applications. For lasers, ultrasound devices, and near-IR imaging, thin film technologies can be used with more advanced sensors and mobile equipment.

Radiation of any kind, including its use in the medical field such as for

diagnostics, treatment, and surgical procedures, as well as in nuclear power systems and constellation-grade satellite cameras, requires extreme attention and care when it comes to micro and nanometer-scale structures of mechanical devices equipped with high-performance nano devices. Extremely thin slices of material, called thin films, which range from a few nanometers to several micrometers in thickness, are now used in a variety of modern technologies including semiconductors, solar cells, and sensors, as well as in protective coatings. However, when considering Iota, aeronautics, and spacefaring, the effect of radiation on thin films remains crucial to investigate thoroughly. To improve electronics' performance, robustness, and dependability in high-radiation situations, it is crucial to comprehend how such complex radiation affects them.

Most experts concentrate on the characteristics of these parts in electrical devices and sensors while researching and analyzing the use of thin films in contemporary kernels.

Fortifying thin films against drastic conditions, or radiation-induced damage, can significantly enhance equipment reliability. Given their main purpose, sensors are continually being changed. However, including micro-geared motors and high-performance liquid cooling often caused thin films to deteriorate much.

1.4. Aim of the Research

We are delving deep in this study to learn how sol-gel spin coating technique affects the microstructure phase makeup surface appearance and crystal quality of Cu-ZnO thin films by varying copper concentrations, spinning fast or slow heating at varying temperatures, and changing solution concentration. Methods include doing a comprehensive examination using X-ray diffraction, which is used to assess the crystal structure, scanning electron microscopy for grain size; atomic force microscopy to assess surface roughness and homogeneity. These phases are vital for figuring out how well the movies will last and stay stable across a range of workplaces.

We will be looking into how well the Cu-ZnO thin films block radiation by comparing their attenuation coefficients with different types of ionizing radiation like gamma rays and X-rays. This will help us see how the band gap shifts the ability to absorb light and how any emission features that are related to defects are affected. Studying these optical properties is very important because it helps us see if these

films are good for things like photo detector applications, lighting up, creating devices, and transparent electronics. We will also be looking into how copper affects the way radiation behaves in the thin film setup. This will help us get a complete picture of why these films are so versatile in their applications.

2. PREVIOUS STUDIES

Particularly fascinating now are copper oxide thin films made up of CuO and Cu2O phases. Thin films are essential for contemporary functional materials since they are inexpensive, environmentally friendly, and readily available for a wide range of applications in the optoelectronic, solar, and sensor fields. Their great capacity to absorb light in the visible spectrum also makes them very appropriate for applications including light sensing and solar energy collection.

Because images may be displayed with the proper colors and in a consistently reliable manner, recent technical breakthroughs have piqued a lot of curiosity in repeating films. The main reason for this is that the color quality is always the same on every screen. Many efforts have been made on copper oxide films lately to raise their light sensitivity. Improving solar panel efficiency and developing light-using chemical energy systems have been particularly dependent on this. These developments enable CuO to be utilized in more applications including energy-harvesting devices, biosensors, and smart sensors. These devices rely on CuO's inherent electrical conductivity and catalytic qualities (Kumar et all., 2022).

Much research conducted between 2015 and 2025 has helped us better grasp the structural, optical, and magnetic properties of copper oxide thin films. Kayani, Iram, Rafi, Riaz, and Naseem (2018), have shown outstanding improvement in the magnetic and optical properties of CuO thin films depending on sol-gel methods with tailored doping and annealing processes. (Kumar et all., 2022) examined the role deposition conditions have in determining the film's microstructure and magnetic response using chemical vapor deposition (CVD), so exposing critical dependencies on grain orientation and border behavior. (Nayak et all., 2023) moved the next step by using PLD and ion doping to create Cu_2O/ZnO heterostructures. This significantly improved charge transport and optical absorption, which in turn significantly improved the performance of solar cells.

(Jagadish et all., 2024) then examined how thermal annealing affected DC-sputtered CuO thin films, finding that phase purity in ITO/CuO/Al Schottky devices improved together with diode performance in general. Taken together, these investigations show that more engineering studies back the development of CuO thin films for possible use in nanoelectronics, sensors, and solar energy systems in future high-tech fields.

Copper oxide thin films are commonly utilized in a range of applications from solar energy to sensors and medical systems due to their ideal bandgap value (1.2–2.2 eV) and semiconducting nature. Their optical and electronic versatility positions them for some functional applications. Cu_2O and CuO are ideal absorber layers for solar cells given their perfect band alignment, accessibility, and renewability. (Arunodaya et all., 2023) achieved unprecedented performance enhancement in Cu_2O/ZnO heterojunction solar cells by modulating the Zn^{2+} ion concentration from 0.8% to 1.5% improvement. While in a limited way, these developments imply that CuO-based materials potentially can offer low-cost and renewable energy sources.

Besides photovoltaic devices, copper oxide thin films find other uses in gas sensing, especially NO_2, CO, and H_2 sensing due to their room temperature stability and high sensitivity. CuO thin films can also be used as high refractive index and transparent anti-reflective films for use in lens and solar collector applications. CuO is used as a p-type semiconductor material for use in electronic devices' transistors and logic gate circuits. Biomedically, biocompatibility and antimicrobial films have also gained their applications in sensing platforms and hygienic coatings which were found effective against bacteria such as S. aureus and E. coli (Du et all., 2022).

techniques have also been upgraded, as discussed by (Kayani et all., 2018), where more than 50% enhancement of photo response of sensors was noted for Zn-doped CuO films. (Buzok et all., 2024) presented the application of cobalt doping to carrier concentration and optical absorption—a finding that can be applied to CuO systems. The emphasis on low-temperature preparation routes like electrodeposition and sol-gel allowed for industrial scale upscaling without allowing loss of control over the nanostructure morphology (Kuriakose et all., 2015). Gamma radiation resistance of CuO films and their blend with biodegradable polymers for antimicrobial application also increases in biomedical and nuclear applications (Devi et all., 2022).

Despite such a breakthrough, challenge towards full commercialization of copper oxide thin films persist. One of them is phase purity control between CuO and Cu_2O because their extremely close thermodynamic properties can yield undesirable mixed-phase products that can hamper device performance and are of potential toxicity (Abraham et all., 2023)). It is difficult to achieve a homogeneous morphology of the surface; grain boundaries and roughness are charge recombination sites, which reduce carrier lifetime (Numanoğlu et all., 2022). Homogeneous doping

control is technologically difficult with secondary phases emerging as impurities during processing (Abraham et all., 2023). Environmental degradation due to oxidation or exposure to water also leads to difficulty in long-term stability (Kumar et all., 2022). Besides that, while methods like ALD and PLD yield high-quality films, such are even too costly and difficult to up-scale (Chen et all., 2018).

Upcoming research needs to push past these boundaries in innovative ways. Hybrid deposition techniques encompass a couple of methods - for instance things like plasma-enhanced spray pyrolysis & solution-processing ALD - which can do cost-effective & conformal film deposition (Xiang et all., 2024). We'll also be looking at the fabrication of nano-structured shapes like nanotubes and nanowires, to see if that can improve charge transport & photocatalytic activity (Chen et all., 2011). We'll be using real-time monitoring techniques like XRD & spectroscopic ellipsometry to keep an eye on phases and doping as the synthesis happens (Singh et all., 2023). And to make these new materials more durable we'll need to improve their environmental stability through surface modification, passivation and encapsulation (Numanoğlu et all., 2022). To speed up the discovery of perfect dopants and heterostructures and bridge the gaps between experiments and theories - we can use computer software like DFT & machine learning (Abraham et all., 2023)

Briefly, CuO and Cu_2O thin films are economical and eco-friendly promising semiconductor material. Grappling with preparation approaches, structure, and functional ability has paved new grounds in various disciplines of technology, including photovoltaics, sensors, and catalysis. Yet, there is a need for development to transmute the major hurdles, i.e., phase control, doping homogeneity, long-term stability, and cost-efficient scalability. Continued interdisciplinary research—encompassing materials science, device engineering, and computational modeling—is vital to transform copper oxide thin films from laboratory innovations into practical, real-world technologies suitable for next-generation applications.

3. MATERIALS AND METHODS

3.1. Materials

The materials for preparing the CZO thin films for the sol-gel process have been given in Table 3.1.

Table 3.1. List of chemicals used in this study.

Chemical Name	Chemical Formula	Purpose / Usage
Zinc acetate dihydrate	$Zn(CH_3COO)_2 \cdot 2H_2O$	Fixed main material for sol-gel production (ZnO source)
Monoethanolamide	$HOCH_2CH_2NH_2$	Solvent: added drop by drop in each sol
Isopropanol	C_3H_8O	Solvent in sol preparation; used for cleaning glass substrates (ultrasonic bath)
Pure Water (Distilled H_2O)	H_2O	Used in cleaning glass substrates (ultrasonic bath)
Acetone	C_3H_6O	Used in cleaning glass substrates (ultrasonic bath)
Nikotinik hidrazit		Used in the synthesis of copper compound
2-hidroksinaftaldehit		Used in the synthesis of copper compound

Also, the devices used in the preparation of thin film coatings and the tests of structural, and optical analysis of the prepared coatings, the models of the devices and their purposes of use have been given in table 3.2.

Table 3.1. Devices used in the study

Device Name	Device Brand	Purpose of Use
Magnetic stirrer	ISOLAB	Preparation of sols and gels
Ultrasonic bath	ISOLAB	Cleaning glass substrates
Spin coating device	POLOS spin coater	Production of thin films
Oven	MSE Furnace	Annealing of produced films
Precision balance	RADWAG	Weighing
SEM (Scanning Electron Microscope)	Zeiss Evo 50	Structural examination
UV-Vis Spectrophotometer	PG Instruments Ltd	Determination of optical properties
XRD (X-ray Diffraction)	Rigaku Ultima III	Structural examination and phase determination
FTIR Spectrophotometer	Perkin Elmer Brand 400 FTIR	Structural examination
Raman	WITec Alpha M+	Structural examination
Coating device	EMS-550	Gold coating before SEM examination
Radiation shielding detector	ULEGe detector (Mirion Tech.)	Determination of radiation shielding properties

3.1.1. Copper (II) Acetate Monohydrate

Copper (II) acetate monohydrate ($Cu(CH_3COO)_2 \cdot H_2O$) is used as the copper precursor. Copper acetate is a commonly used precursor for sol-gel processing because it is easily soluble in organic solvents and can provide a stable source of copper ions for the formation of copper oxide.

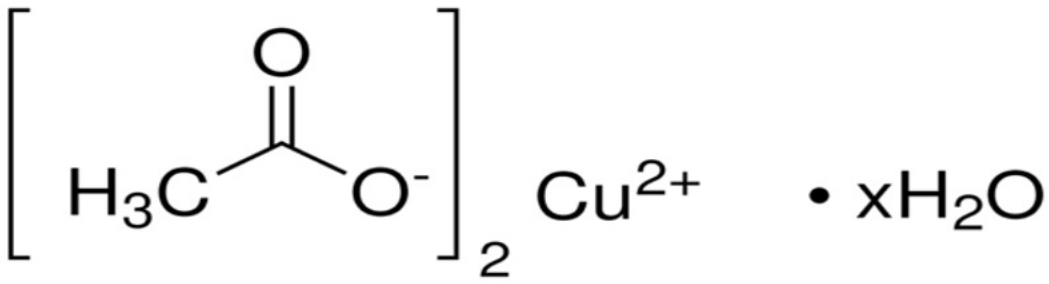

Figure 3.10. Copper (II) acetate 99.99 trace metals 6046-93-1

3.1.2. Zinc Acetate Dehydrate

Zinc acetate dehydrate ($Zn(CH_3COO)_2 \cdot 2H_2O$) serves as the zinc precursor. Zinc acetate is favored because of its high solubility in ethanol and its ability to form

a stable sol during the sol-gel process. It is a well-known precursor to produce transparent conducting oxide films, including zinc oxide and its doped variants.

3.2. Methods

3.2.1. Synthesis Procedure of Copper Complexes

N-((2-hydroxynaphthalen-1-yl) methylene) nicotine hydrazide ligand (L) was synthesized according to the method reported in the literature (Figure 3.1) (Soğukömeroğulları et all., 2022). Nicotinic hydrazide (1) mmol,

0.137 g) was taken into a flask and dissolved in 20 mL ethanol. 2-hydroxynaphthaldehyde (1 mmol, 0.172 g) was added dropwise. It was refluxed for 1 hour under reflux. The solvent was removed from the evaporator. The obtained solid was washed several times in ethanol and diethyl ether and dried in a desiccator. ((2-hydroxynaphthalen-1-yl) methylene) nicotin hydrazide ligand (L) was synthesized according to the method reported in the literature (Figure 3.1) (Soğukömeroğulları et all., 2022). Nicotinic hydrazide (1) mmol, 0.137 g) was taken into a flask and dissolved in 20 mL ethanol. 2-hydroxynaphthaldehyde (1 mmol, 0.172 g) was added dropwise. It was refluxed for 1 hour under reflux. The solvent was removed from the evaporator. The obtained solid was washed several times in ethanol and diethyl ether and dried in a desiccator.

Figure 3.11. N-((2-hydroxynaphthalen-1-yl) methylene) nicotin hydrazide ligand.

After then, 15 mL of ethanol solution of 0.5 mmol of metal acetate salt was added to 20 mL of ethanol solution of 1 mmol of ligand in a beaker. A sudden colour change was observed with the addition of metal salt to the ligand solution. The reaction medium was stirred with a magnetic stirrer at 65 °C for 30 minutes. The reaction was terminated when precipitation occurred. The precipitated material was filtered, washed several times with cold water, methanol and diethyl ether. The compound was purified in ethyl alcohol and dried in a desiccator (Figure 3.2).

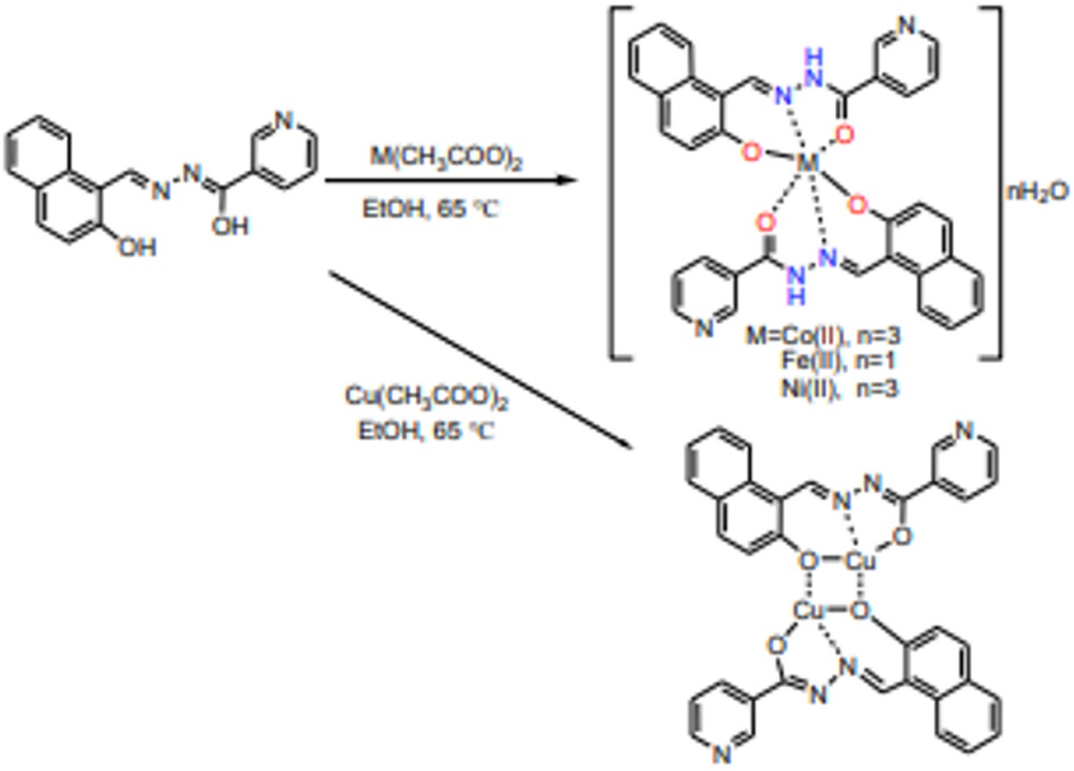

Figure 3.12. Synthesize of copper complex.

The obtained information's during form of copper complex is given in Table 3.2.

Table 3.2. Information of copper complex.

Colour	dark brown
Yield:	0.592 g (85 %)
Decomposed	above 360 °C
IR, (ATR) v, cm-1:	3079 (C-H) aromatic, 2988 (C-H) aliphatic, 1609, 1585 (C=N), 517 (M-N), 462 (M-O);
UV-Vis (DMF) λmax (Abs):	490 (0.187), 465 (0.195), 450 (0.158), 380 (0.369), 365 (0.413), 355 (0.374), 325 (0.428), 320 (0.315), 295 (0.239), 265 (0.473) nm
μeff:	1.61 B.M.
Conductivity 2x10-5 M DMF (ΛM):	2.61 μS/cm.
Theoretical:	C34H22Cu2N6O4 (705.67); C, 57.87; H, 3.14; N, 11.91 %. Found: C, 58.50; H, 3.72; N, 12.48%

3.2.2. Production of Copper Zinc Oxide Thin Films

The synthesis of CZO thin films involves the preparation of a sol-gel solution, followed by spin coating and subsequent thermal treatment (annealing) to crystallize the films.

3.2.2.1. Sol Preparation

The sol-gel process begins with the preparation of a homogeneous solution. Copper acetate monohydrate and zinc acetate dehydrate are dissolved in ethanol in varying molar ratios to achieve the desired copper-to-zinc concentration (e.g., Cu:Zn= 1:1, 2:1, etc.). The solution is stirred for 2 hours at room temperature to ensure complete dissolution of the precursors and uniformity in the sol.

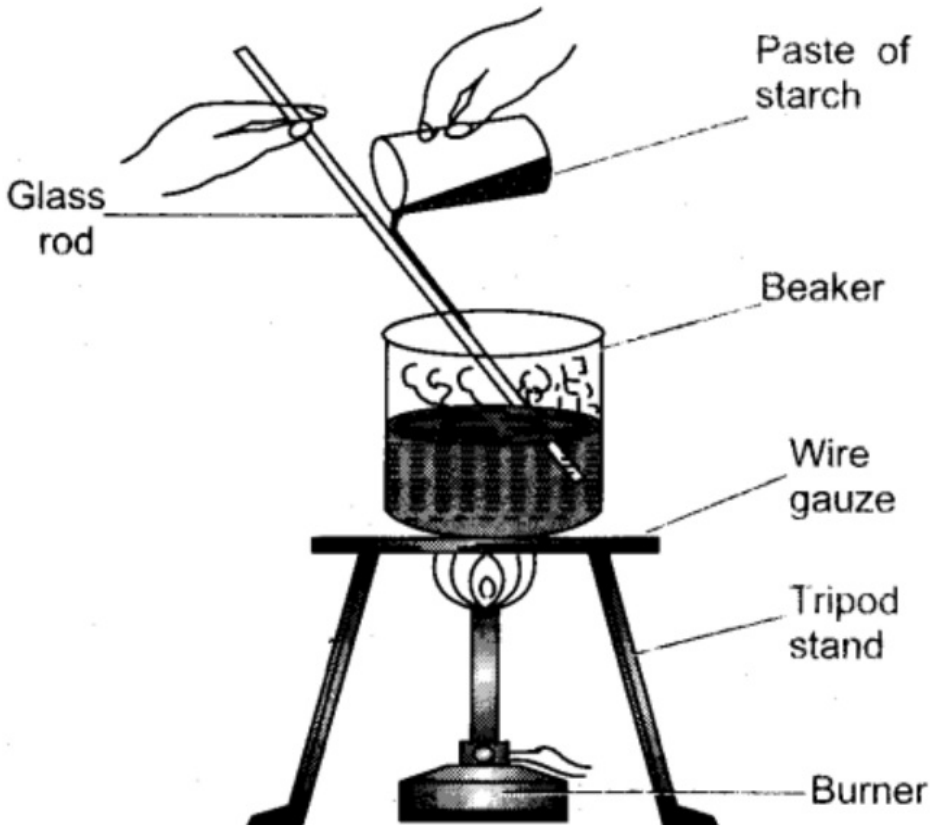

Figure 3.13. To Prepare Colloidal Solution (sol) of Starch - Infinity Learn

3.2.2.2. Spin Coating Process

The sol prepared is deposited onto clean glass or silicon substrates by spin coating. Spin coating is a widely used method for producing thin films due to its

ability to create uniform films with controlled thickness. The deposition process involves the following steps:

A. Substrate Cleaning: The substrates are cleaned by rinsing them in deionized water, followed by ethanol, and then dried with a nitrogen gun. This ensures the removal of organic contaminants and particles on the substrate surface.

B. Spin Coating: 50µL of the sol were dispensed onto the center of the substrate. The substrate was then rapidly rotated at a predetermined speed of 3000 rpm to spread the sol uniformly across the surface.

C. Drying: After spin coating, the film is subjected to a short drying step to evaporate the solvent (ethanol) and form a gel-like structure. This step typically takes place at room temperature or in an oven at temperatures between 200°C.

D. Annealing (Thermal Treatment): The spin-coated films were annealed to improve crystallinity, remove organic residues, and form stable copper zinc oxide (CZO) films. Annealing is performed in a furnace at 500 °C for 2 hours.

3.2.3. Characterization of CZO Thin Films

To assess the structural, optical, and radiation properties of the CZO thin films, a variety of characterization techniques employed.

3.2.3.1. Structural and Optical Characterization

CZO films were checked with XRD to see how they make crystals and what phase they are in. From the pattern made when they diffract, you can tell the phase (such as CuO, ZnO, or CZO), how they lean, and how big the grains are on average. XRD was done using a Rigaku Dmax 2000 with CuKα radiation (λ = 1.5406 Å) at a speed of 0.02° per sec from 20° to 80° in 2θ. The laser from Erciyes U. In Ernam was used for Raman with 532 nm and 785 nm wavelengths. The CZO films were looked at with SEM to see their surface detail and microstructure. This was done with a JEOL SEM at Hübtam.

The optical traits of CZO films were studied with UV-Vis. They used a spectrometer from Perkin Elmer Lambda 950 to record how much light they let pass through, how much they absorb, and their bandgap in the 200–800 nm range. The bandgap was found with the Tauc plot from the absorption edge.

3.2.3.2. Radiation Shielding and Anti-Reflective Characteristics

In last long hours, copper oxide lean films for anti-glare and radiation cover uses have made so much progress because the materials have amazing electron band structures, many nuclear numbers (say for example, Cu), and great optical levels. Copper oxide thin films have shown to be very good as a cover for many types of radiation like gamma and UV rays, making it great for use in aircraft, health gadgets, and atomic labs. (Demircan et all., 2023) studied move metal doped ZnO lean films, such as Co and Cu doped, and found that these dopants made the straight constriction ratio and mass weakening ability of the films better, which then made them good for shielding radiation. Also, (Hamel et all., 2017) said that Cu doped ZnO thin films kept their old stability and optical clearness even after getting gamma radiation doses up to 10 kGy, which is like the durability in bad places. The anti-reflectivity properties of CuO and Cu_2O lean films are also promising. The films themselves have high refractive index list and absorbance in the apparent and near-infrared spectral range, which minimizes reflectance upon deposition on photovoltaic or optical substrates. (Caglar et all., 2012) described that sol-gel-deposited Cu-doped ZnO films have demonstrated reflectance decreases of up to 45% compared to undoped ZnO films. These characteristics are highly useful in enhancing light harvesting in solar powered cells in such a manner as to improve their overall control change efficiency. In this regard, (Yang et all., 2013)researched multilayer CuO-based coatings as a glass surface anti-reflective coating with enhanced sun-based transmission and decreased glare, particularly when movies were fortified at temperatures above 400 °C.

Additionally, radiation-induced imperfection resistance of CuO lean films was researched in depth. (Gupta et all., 2014) illustrated that Cu-doped ZnO films essentially quenched surface reflection while producing more than 80% transmittance in the unmistakable range, rendering them well-suited for anti-glare screen shields as well as camera lenses.

Usually, the two functions of CuO lean films as radiation shield and anti-reflective material open new frontiers in energy-saving, multi-functional films. The developments foreshadow a future where copper oxide lean films not only kept sensitive equipment intact but also optimized advanced vitality collection and image

display in other sectors.

3.2.3.3. X- and Gamma Ray Absorption

Using a VEX source, gamma radiation tests are performed to examine the radiation characteristics of the CZO thin films. Researchers at the Prof. Dr. Wolf Weyrich High Energy Spectroscopy Research Laboratory studied the radiation shielding characteristics of thin films.

Department of Physics, Faculty of Science, Atatürk University. Fig. 3.5a illustrates the experimental configuration employed for photon attenuation analysis, comprising a Variable Energy X-ray (VEX) source, sample, and a semiconductor-based radiation detector. The VEX system can generate characteristic X-rays with distinct energies, depending on the secondary target material irradiated. These secondary targets were activated using a 59.54 keV gamma emission from an Am-241 source with an activity of 3×10^7 Bq. Materials including copper (Cu), rubidium (Rb), molybdenum (Mo), silver (Ag), barium (Ba), and terbium (Tb) were selected as secondary targets. The characteristic K X-rays emitted from these targets (notably from Rb, Mo, Ag, and Tb) were directed onto the CZO thin film samples under investigation.

Table 3.4 summarizes the specific X-ray energies produced. Photon intensities before and after interaction with the samples were recorded using an Ultra-Low Energy Germanium (ULEGe) detector. Each spectral measurement was conducted over a 3600 second acquisition period. An example transmission spectrum for the CuZnO5 sample is shown on Fig 4.6. All attenuation parameters were derived based on the Lambert-Beer law. The radiation shielding parameters as linear and mass attenuation coefficients (LAC and MAC), mean free path (MFP), half-value layer (HVL) and effective atomic numbers (Zeff) were measured in the energy region 13.37-59.54 keV of CZO thin films.

Table 3.3. X-ray emission energies of radioactive VEX source.

Selected target	**Energy (keV)**	
	K_α	K_β
Rb	13.37	14.97
Mo	17.44	19.63
Ag	22.10	24.99
Tb	43.74 ($K_{\alpha 2}$) and 44.48 ($K_{\alpha 1}$)	50.38 ($K_{\beta 1}$) and 51.71 ($K_{\beta 2}$)

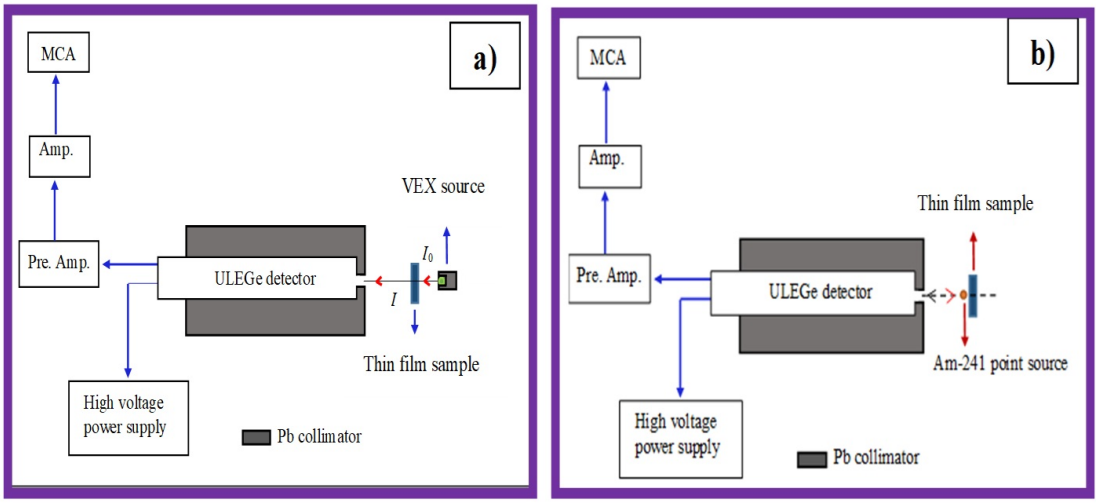

Figure 3.14. a) Absorption geometry, b) Backscattering geometry in gamma spectroscopy.

b) Determination of Albedo parameters

Fig. 3.6 illustrates the experimental arrangement implemented for the determination of albedo parameters via photon backscattering. In this configuration, CZO thin films were exposed to monoenergetic photons with an energy of 59.54 keV, emitted by an Americium-241 source. The setup was designed to capture photons scattered at a backscattering angle of 180°, which were subsequently registered by ULEGe detector. The resulting energy spectra were systematically examined to identify and differentiate the peaks associated with Rayleigh (coherent) and Compton (incoherent) scattering events. Each measurement cycle was conducted over a 7200 second acquisition interval. Comprehensive methodological details and all relevant parameters required for the computation of albedo values can be found in (Yılmaz et all., 2020). Detector photo peak efficiency were determined by measuring the X-ray yields from spectroscopically pure targets Co, Zn, Y, Mo Ba, Dy, Lu, Au and Pb. The typical scattering spectra of some thin samples were given in Fig. 3.7.

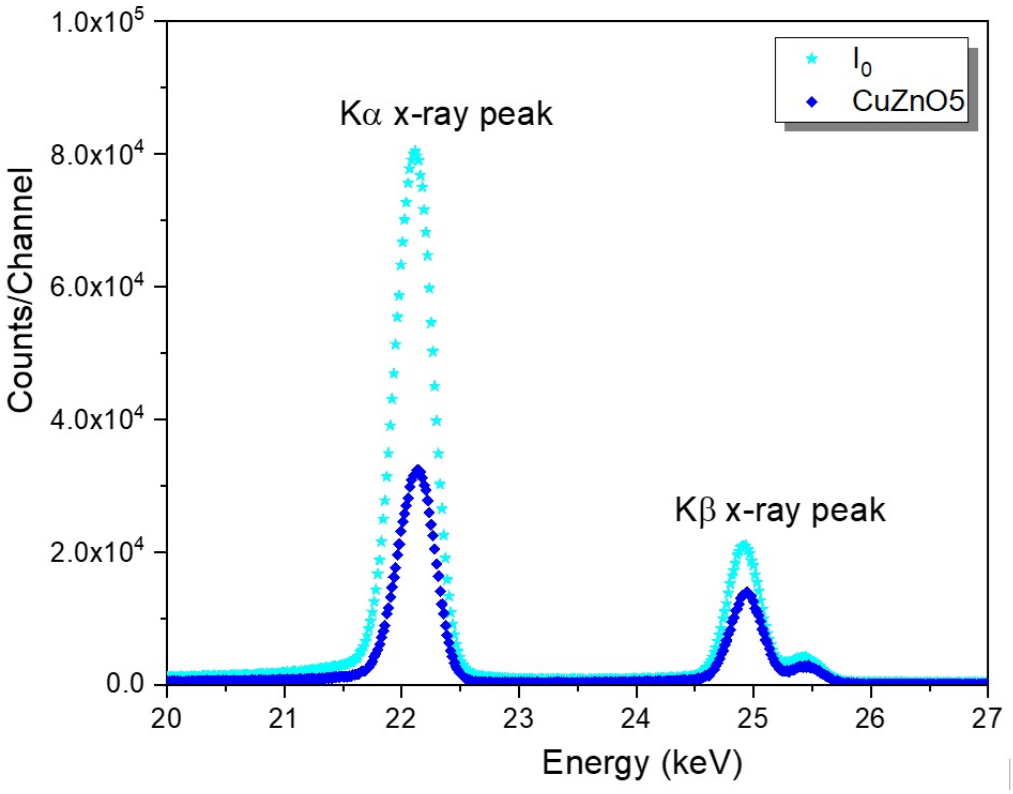

Figure 3.15. The transmisson spectra of CuZnO5 for Ag K x-rays from VEX source.

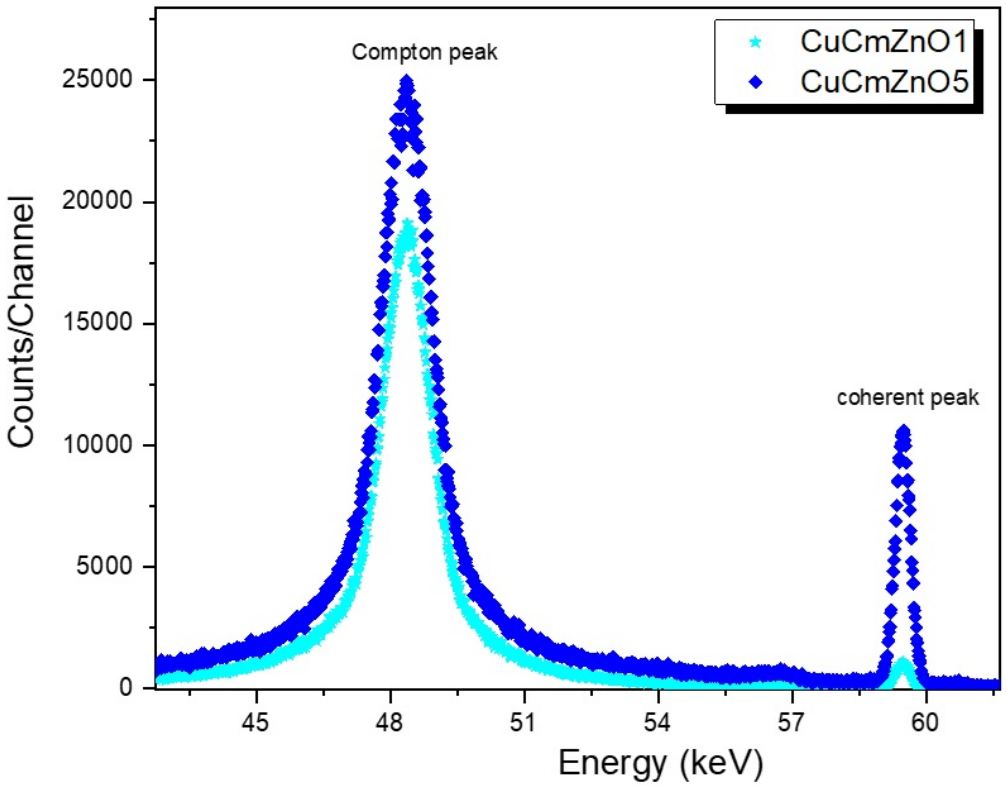

Figure 3.16. The scattering spectra of CuCmZnO1 and CuCmZnO5.

c) Neutron Attenuation

The effectiveness of the materials in attenuating fast neutrons was assessed by measuring the neutron equivalent dose rates. These measurements were carried out using a BF_3-filled proportional counter coupled with a standard Americium-Beryllium (Am-Be) neutron source. A comprehensive depiction of the experimental setup is provided on Fig. 3.8. All mathematical expressions and theoretical formulations employed in the analysis are systematically compiled in Table 3.4.

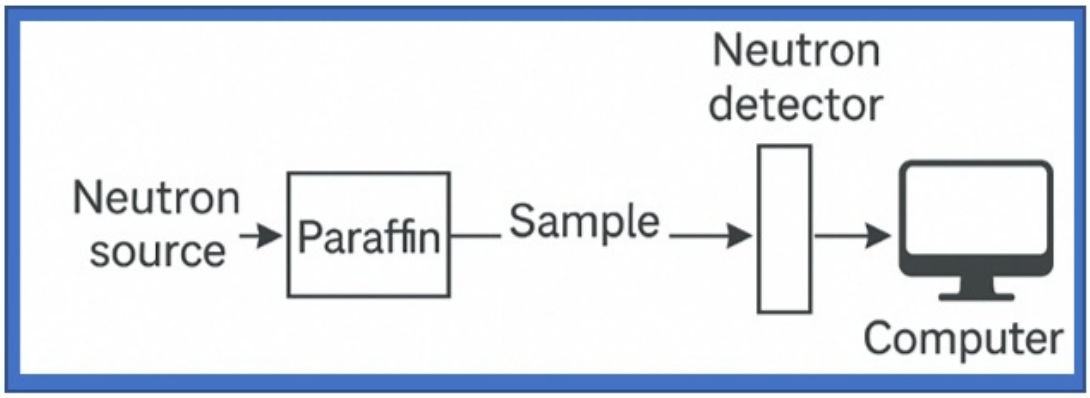

Figure 3.17. The experimental geometry for neutron dose measurements.

Parameters	Equations	Descriptions
Linear attenuation coefficients, (LAC, cm^2/g)[1]	$\mu = ln(I_0/I)/t$	I_0 and I are the intensities of the incident photons and those passing through the absorber, respectively.
Mass attenuation coefficients, (MAC, cm^2/g)[1]	$\mu_m = ln(I_0/I)/\rho t$	ρ is the density and t is thickness.
Mean free path, (MFP, cm)[1]	$MFP = 1/\mu$	μ is the linear attenuation coefficient (1/cm).
Half value thickness, (HVL, cm)[1]	$HVL = 0.693/\mu$	μ is the linear attenuation coefficient (1/cm).
Effective atomic number[1]	$Z_{eff} = \sigma_{t,a}/\sigma_{t,e}$	The total electronic cross section is $\sigma_{t,e}$ and the total atomic cross section is $\sigma_{t,a}$
Albedo number[2]	$A_N = \left[\frac{N_{Comp}/\varepsilon(E_{Comp})}{(N_{coh}/\varepsilon(E_{coh}))(1/d\Omega)(1/2)}\right]$	$d\Omega$ is the solid angle, N_{Comp} and N_{coh} are the areas of Compton and coherent scattered peaks. The photo-peak efficiencies are $\varepsilon(E_{Comp})$ and $\varepsilon(E_{coh})$ in Compton and coherent scattered energies.
Albedo enegy[2]	$A_E = [E_s/E]A_N$	E_{Comp} and E are the energies of the in Compton and coherent scattered energies.
Albedo dose[2]	$A_D = \left[\sigma_a(E_{Comp})/\sigma_a(E)\right]A_E$	$\sigma_a(E_{Comp})$ and $\sigma_a(E)$ are the energy absorption coefficients of air for in Compton and coherent scattered energies.
Buildup factor[1]	$I = BI_0e^{-\mu_m \rho t}$	B is build up factor.
Fast neutron removal cross section[3]	$\Sigma_R = \sum_i W_i(\Sigma_{R/\rho})_i$	Fast neutron removal cross section of the ith element is denoted by $\Sigma_{R/\rho}$, while W_i represents its partial density.
Fast neutron macroscopic cross section[4]	$\Sigma_R = ln(I_0/I)/t$	I_0 and I are incident and transmitted intensities for fast neutrons, respectively, within the energy range of 4 MeV and t is absorber thickness.
Thermal neutron cross section[4]	$\Sigma_R = ln(I_0/I)/t$	Σ_R is the probability of thermal neutrons (25.4 meV) being retained in a unit length of matter.
Mean free path (neutron)	$MFP = 1/\Sigma_R$	MFP is the part travelled by a neutron between two collisions.
Half value thickness (neutron)	$HVL = 1/\Sigma_R$	HVL is the thickness of the material that reduces incoming neutron radiation by half.
The absorbed equivalent dose percentage	$(I_0 - I)/I_0 \times 100$	I_0 and I are the intensities of incident neutrons and those passing through the absorber, respectively.
Neutron attenuation rate	$(1 - I/I_0) \times 100$	I_0 and I are the intensities of the incident neutrons and those passing through

Figure 3.18. The used equations and definitions for the present study.

1. The EpiXS software program is used to calculate theoretical values (Hila et all., 2021)
2. The calculating procedure of albedo numbers is available from us

previous work (Ivanova et all., 2025).

3. Theoretical values are calculated using the Phy-X software package (Sakar et all., 2024).
4. Theoretical values are calculated using the NGcal software package (Seredin et all., 2021).

4. FINDINGS

4.1. X-Ray Diffraction

The XRD patterns of the ZnCuO thin films (0, 1, 3 and 5%) annealed at 500°C can be seen in Figure 4.1. All the prepared ZnO films have a hexagonal wurtzite crystal structure and consist of (100), (002), (101), (102), (103), (110) (112) and (201) planes. The XRD results show that the samples have a high crystalline phase and that the addition of copper acts as a substituent dopant in ZnO without changing the wurtzite crystal structure. While the intensity of the (100), (002) and (101) planes is higher in the diffraction pattern of the pure sample, a decrease in the intensity of these planes occurred with the inclusion of Cu and Cu complex.

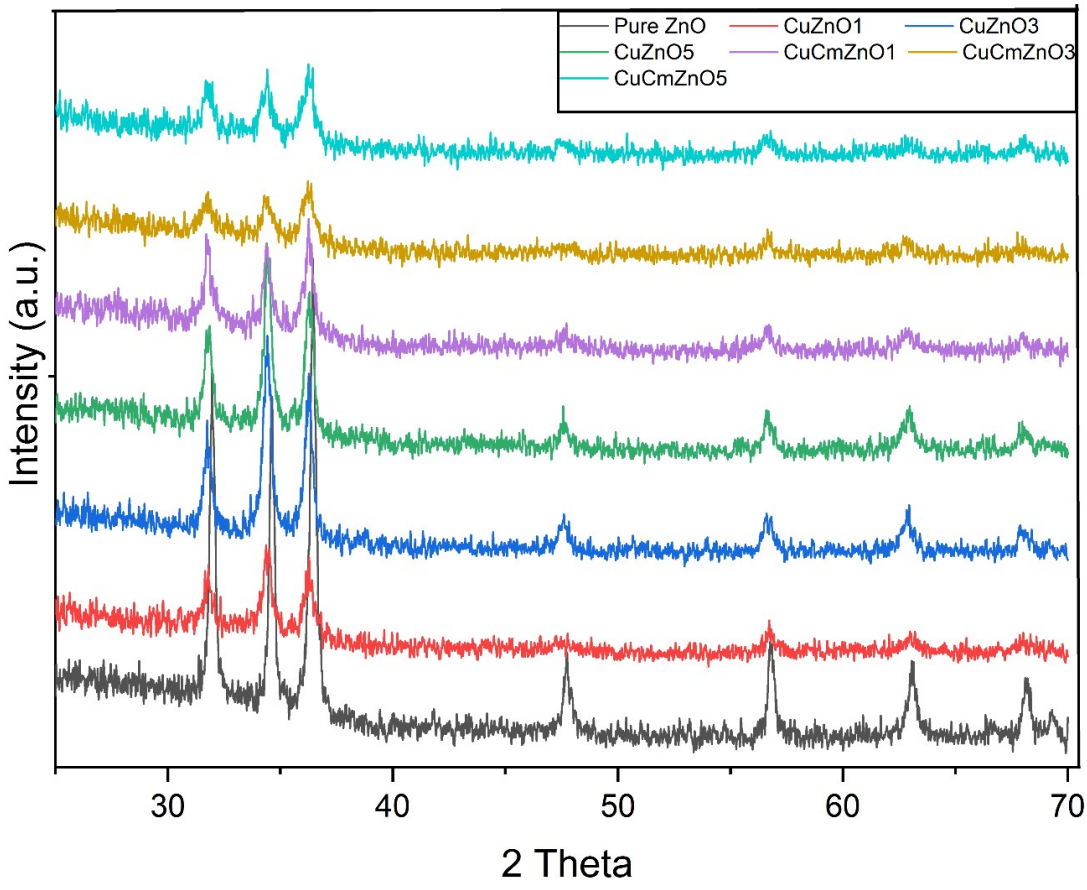

Figure 4.7. Figure 4.1. XRD diffraction patterns of Cu:ZnO films

When the XRD graph is examined, it is seen that the Cu doping causes a decrease in the intensity of the (100), (002) and (101) planes compared to the pure. As the Cu doping increases, the intensity of the diffraction planes increases. While it is lower by 1%, it is slightly higher than 5%. In addition, the Cu doping shows growth in the (002) direction. As for the copper complex additive, it has been seen

that the intensity has decreased depending on copper complex. 1% has bigger intensity than 5% copper complex. In addition, a shift towards lower angles was observed in these planes due to copper doping. These shifts occur due to the ionization of ZnO and external/internal stress component in the films. Some properties of CZO thin films and weight fraction (%) of compounds were given in Table 4.1 and Table 4.2, respectively.

Table 4.1. Table 4.1. Unit cell parameters, crystallite size values and thickness values of the prepared films of Cu:ZnO films

Sample code	a (Å)	c (Å)	Grain size (nm)	Film thickness (nm)	Density (g/cm^3)
Pure	3.249	5.207	30	300	3.25
CuZnO1	3.248	5.206	28	310	2.36
CuZnO3	3.247	5.204	26	320	2.93
CuZnO5	3.245	5.201	24	330	3.19
CuCmZnO1	3.243	5.2	22	340	1.95
CuCmZnO3	3.242	5.198	20	350	1.99
CuCmZnO5	3.24	5.195	18	360	2.00

Table 4.2. Table 4.2. Sample code and weight fraction (%) of compounds in CZO thin films.

Sample code	**$CuC_4H_8O_5$**	**$ZnC_4H_{10}O_6$**	**$C_{34}H_{22}Cu_2N_6O_4$**
Pure	-	100	-
CuZnO1	0.476	0.524	-
CuZnO3	0.732	0.268	-
CuZnO5	0.816	0.184	-
CuCmZnO1	-	0.237	0.763
CuCmZnO3	-	0.094	0.906
CuCmZnO5	-	0.060	0.940

Unit cell parameters were calculated using the equation from the (100) and (002) planes.

$$\frac{1}{d^2} = \frac{4}{3}\left(\frac{h^2 + hk + k^2}{a^2}\right) + \frac{1^2}{c^2} \tag{4.1}$$

The unit-cell parameters for all films were approximately a = 3.23 Å and c = 5.18 Å. These values are very close to the hexagonal wurtzite structure (Gürses, 2020). The grain size for the films was obtained at the level of 25.41-64.65 nm.

4.2. UV-VIS Analysis of Cu and Cu Complex Doped Films

The UV-Vis absorption spectrum of Cu:ZnO thin films is shown in (Figure 4.2). The pure ZnO has shown band edge at around 395 nm. The copper doped films have shown band edge between 400 and 700 nm. The optical absorption edge showed a shift towards higher wavelengths with increasing copper content.

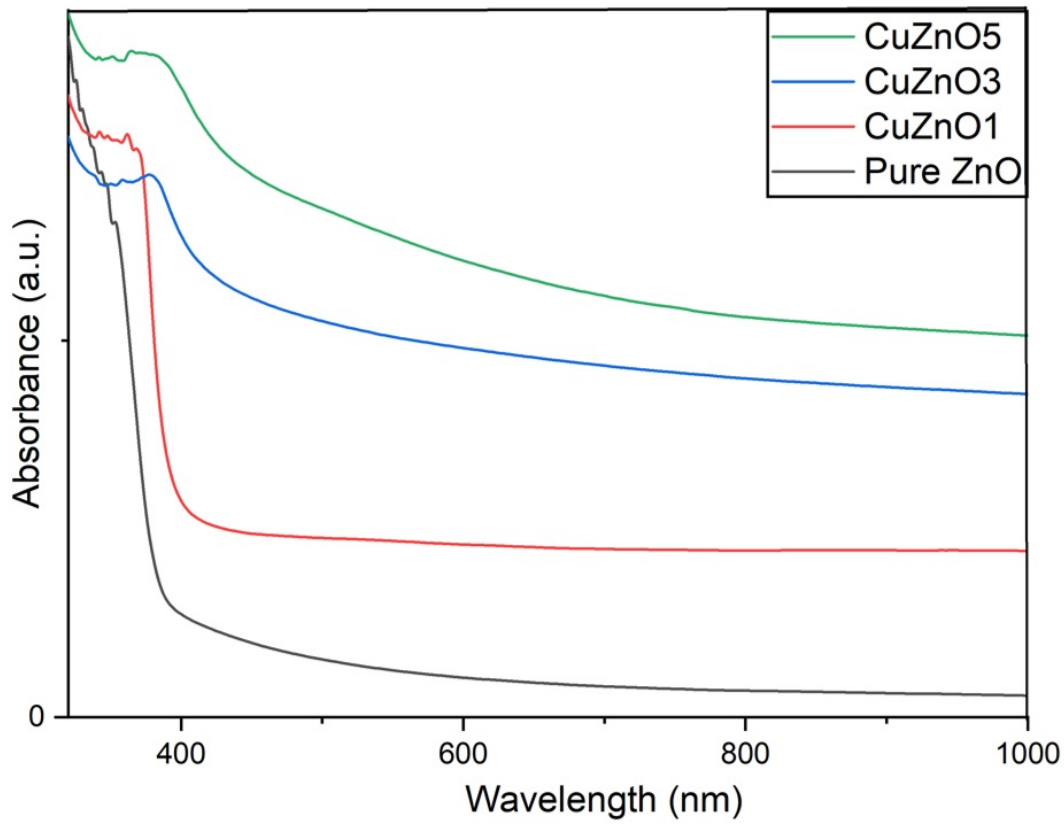

Figure 4.8. UV-Vis absorption spectra of ZnO, Cu:ZnO thin films.

The UV-vis absorption spectra of copper complex doped films have shown a

band edge in the visible range (Figure 4.3). Also, the optical absorption edge showed a shift towards higher wavelengths with increasing copper content.

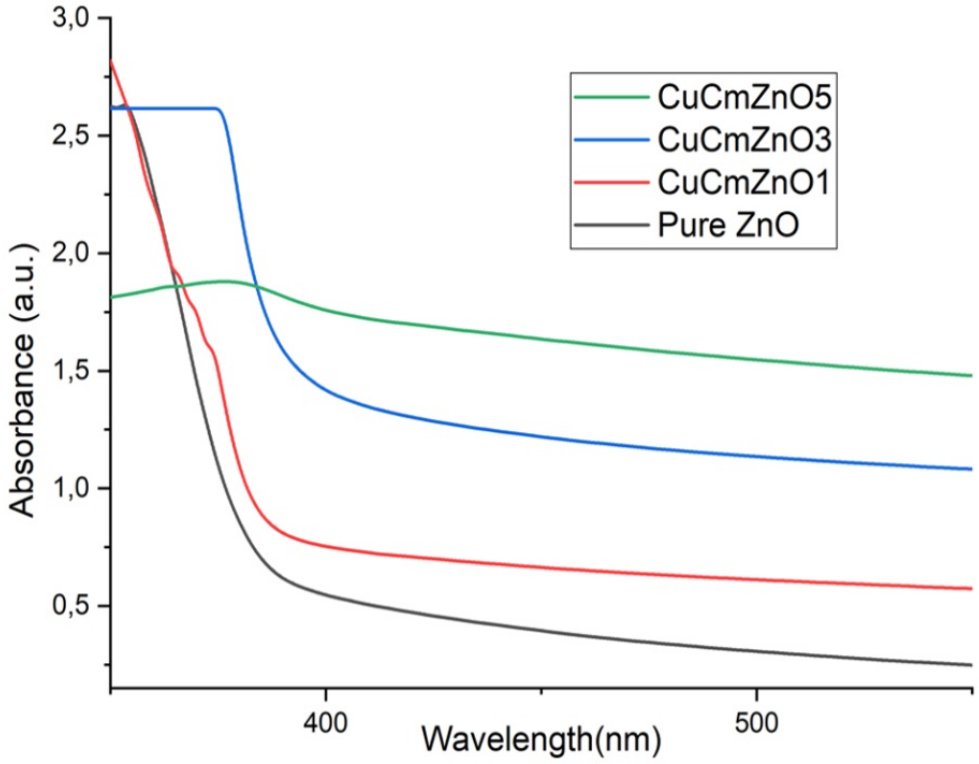

Figure 4.9. UV-Vis absorption spectra of ZnO, ZnO thin films with Cu complex.

Additionally, the optical band gap of ZnO, Cu:ZnO films was calculated using the Tauc model according to equation 1.

$$(Ah\nu)^2 = A(h\upsilon - Eg) \tag{4.2}$$

Here A is a proportionality constant, hν is the photon energy of the incident light, and Eg is the optical band gap.

As shown in Figure 4.4, the band gaps of the films vary between 2.25 and 3.22 eV for pure ZnO and Cu doped ZnO. The optical band gap value decreases depending on copper doping. When copper complex is added, the band gaps obtained for the films are smaller than pure ZnO.

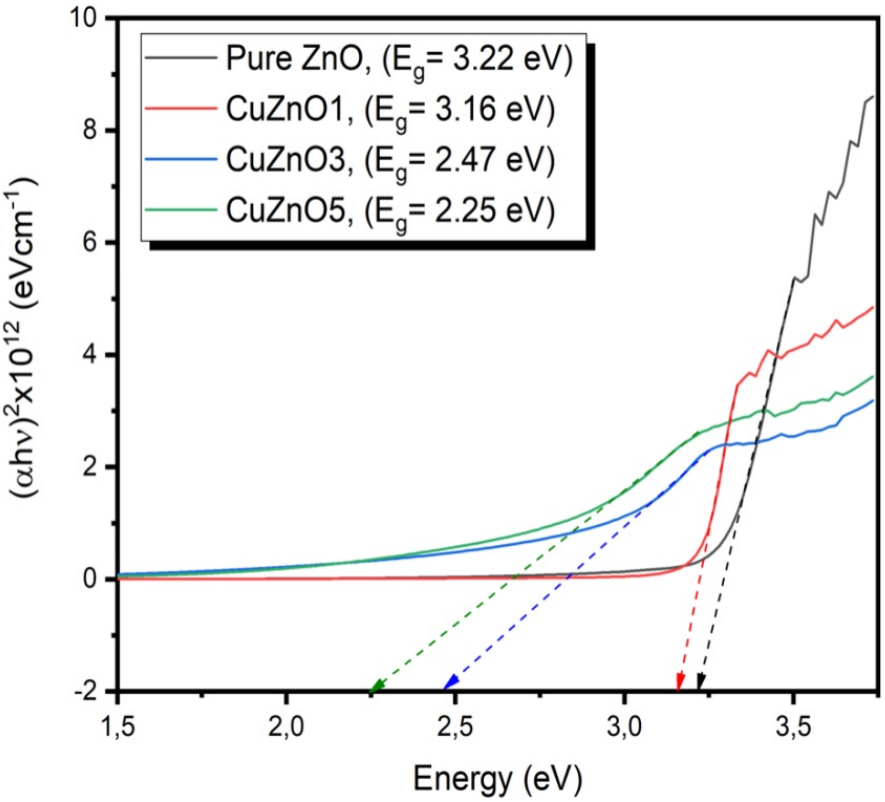

Figure 4.10. Optical band gap of the Cu doped ZnO thin films.

As for films with Cu complex additives, depending on Cu complex doping to ZnO can be seen the same effect. The bandgap values have obtained between 3.22 and 2.98 eV and it has decreased depending on Cu complex doping to ZnO. It has obtained bigger value than Cupper doped ZnO in the same depending on amount in copper complex doped ZnO.

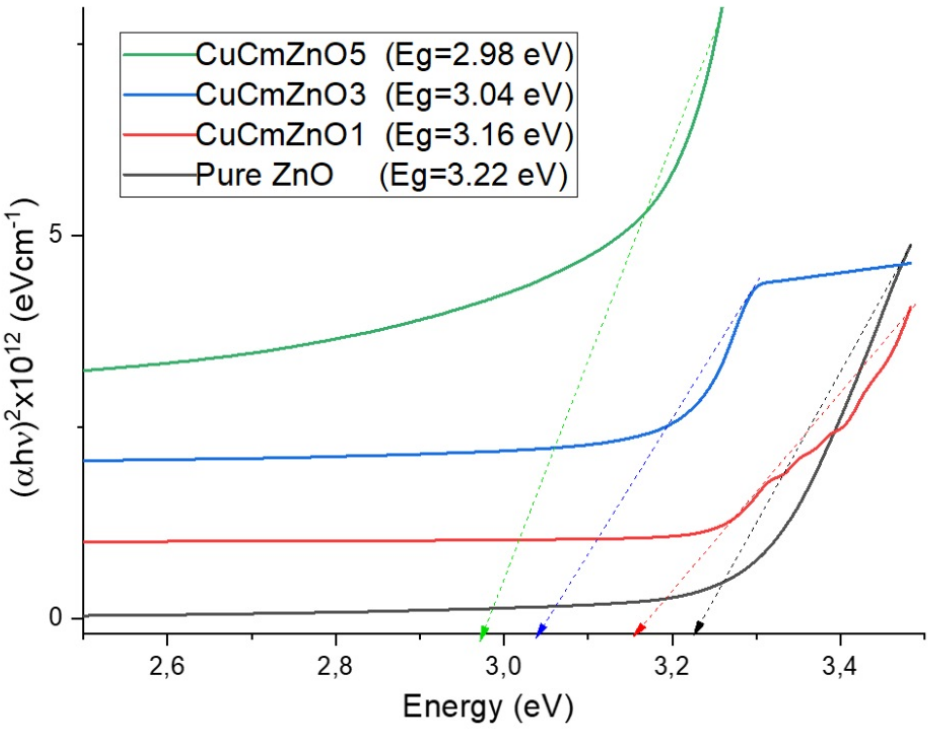

Figure 4.11. Optical band gap of the Cu complex doped ZnO thin films.

The refractive index was calculated using the Hervé and Vandamme formula given in Equation 2 (P. Hervé and Vandamme, (1994)). The refractive index values of Cu:ZnO thin films are given in Table 4.3.

$$n = \sqrt{1 + (\frac{13.6}{Eg + 3.47})^2} \tag{4.3}$$

Here n and Eg are called the refractive index and band gap energy, respectively. The refractive index of ZnO was found to be around 2.39 eV. This value decreased depending on the copper content.

Table 4.3. Band gap and refractive index values of Cu:ZnO thin films

Sample Code	Eg (eV)	n
Pure	3.22	1.85
CuZnO1	3.16	1.87
CuZnO3	2.47	2.3
CuZnO5	2.25	2.47
CuCmZnO1	3.16	1.87
CuCmZnO3	3.04	1.93
CuCmZnO5	2.98	1.96

4.3. Raman Spectra of CuZnO Thin Films

Fig. 4.6 shows the Raman spectra of the ZnO and Cu/Cu complex doped ZnO thin films. Raman spectra of ZnO grown on Si substrates show vibrational modes attributed to a wurtzite structure of ZnO. The spectra reveal peaks at 333 cm-1, 432 cm-1 and 571 cm-1. These modes have corresponding to E2(high)–E2(low), E2(high) and A1(LO)/E1(LO) modes of ZnO, respectively (Kuriakose et all., 2015). The peak at 432 cm-1 is the characteristic E2 (high) of ZnO phonons. This mode is mainly due to the vibration of oxygen atoms and arises from which ensures the good crystal quality (Ansari et all., 2018). The observed four peaks corresponding to ZnO are present in all the samples but are more prominent in samples ZnO and CuZnO1 and this peak diminished in intensity due to the formation of ZnO–CuO nanohybrids and decrease in the crystallinity of ZnO (Kuriakose et all., 2015). The strong peak at 571 cm−1 was caused by the CuO crystals' A1g Raman-allowed mode; the faint peak at 288 cm−1 is attributed to Ag, and 1119 cm−1 refers to the 2Bg mode, which is a Cu–O stretching mode (Jagadish and Kekuda, 2024).

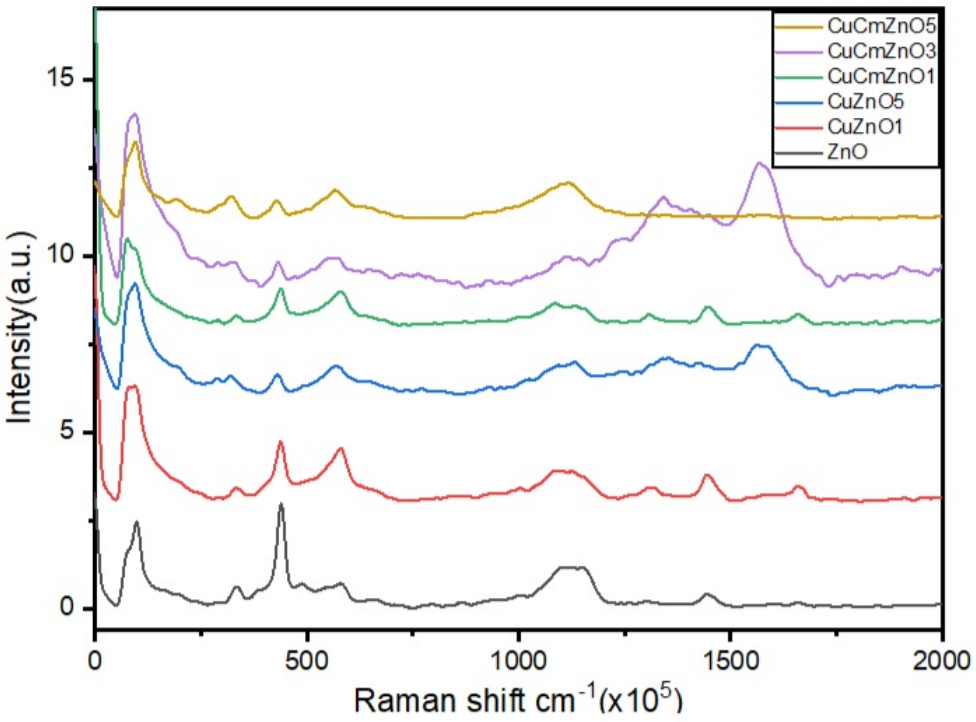

Figure 4.12. Raman shifts of Cu and Cu complex doped ZnO

4.4. Scanning Electron Microscopy and Microstructural Investigation

The surface morphology analyses of the Cu-doped ZnO thin film with different cupper concentration has been performed using a scanning electron microscope (SEM). The microstructure images of thin films are shown in Figure 4.7. In all surface images, it is seen that the coatings are stable and the surfaces have nanofiber-like images. The evaporation of monoethanolamide used as a stabilizer during annealing caused nanofiber-like images to be obtained and is like previous studies (Demircan et al., 2023) ; (Buzok et all., 2024). The roughness has increased with the copper oxide concentration, and the formation of occasional pores and cracks has been observed on all the film surfaces for cu doped ZnO. As for cupper complex dopant, it was observed that continuous films are obtained for all cupper complex doped samples. The as-deposited complex thin film is found to have uniform grains, similar surface morphology reported by (Arunodayaet et all., 2023). The view of Cu complex/ZnO thin films shows that ZnO films are continuous with granular structure.

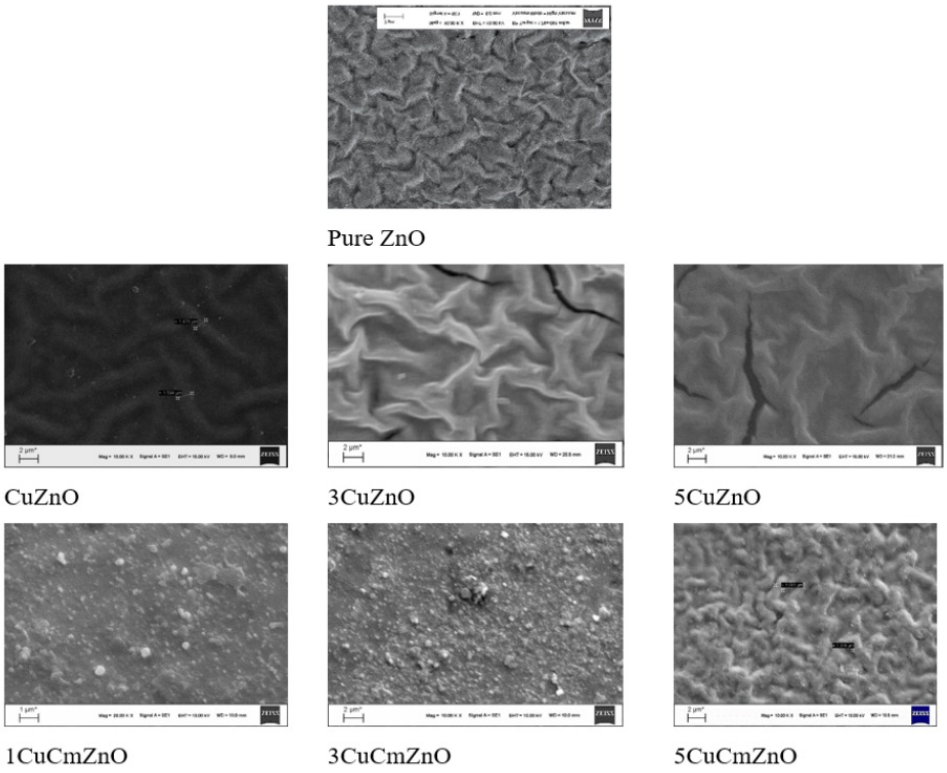

Figure 4.13. SEM image of cupper doped ZnO films

4.5. Radiation Shielding and Anti-Reflective Characteristics

4.5.1. X- and Gamma Ray Absorption

The linear attenuation coefficients (LAC) of CZO thin films were experimentally evaluated and the energy-dependent trends of the LAC were given in

Fig. 4.8. The theoretically and experimentally results for LAC is calculated. The experimental data of LAC exhibited strong alignment with the theoretical estimates, with deviations confined to a narrow interval ranging from approximately 0.82% to 6.10% across the studied energy range (13.37–59.54 keV).

The mass attenuation coefficients (MAC) of CZO thin films were experimentally evaluated and the energy-dependent trends of the MAC were given in Fig 4.10. The theoretical and experimental results for MAC are provided in Table

4.5. As seen from Table 4.5, the experimental data of MAC exhibited strong alignment with the theoretical estimates, with deviations confined to a narrow interval ranging from approximately 0.12% to 5.98% across the studied energy range (13.37–59.54 keV). Measurement uncertainties were maintained below 5.28%.

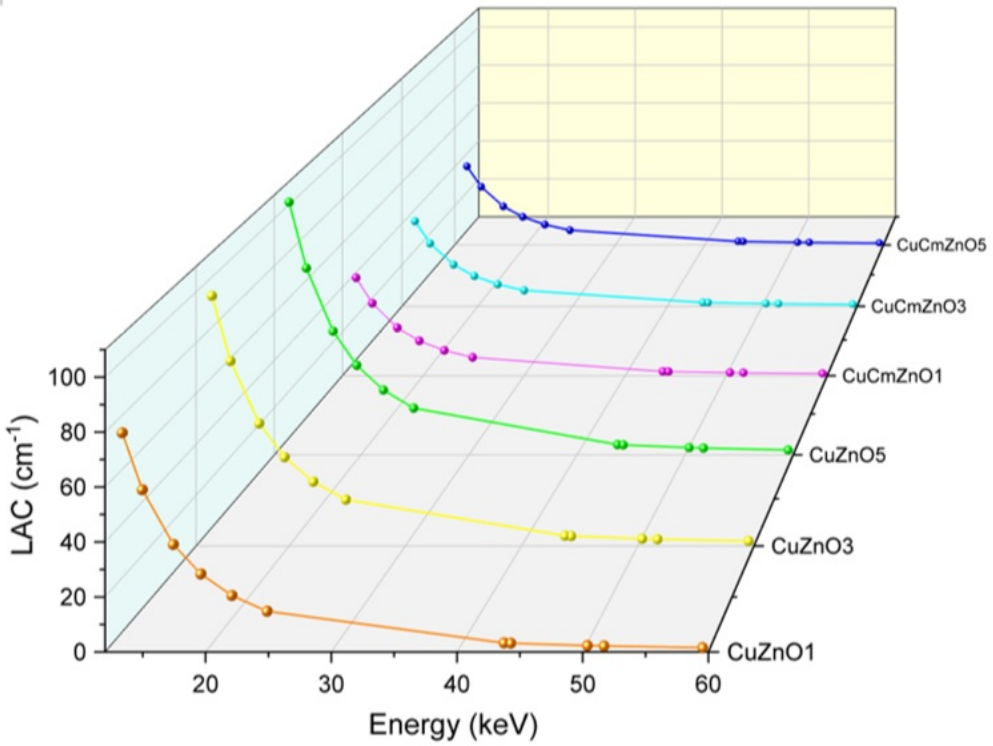

Figure 4.14. LAC values of CZO films.

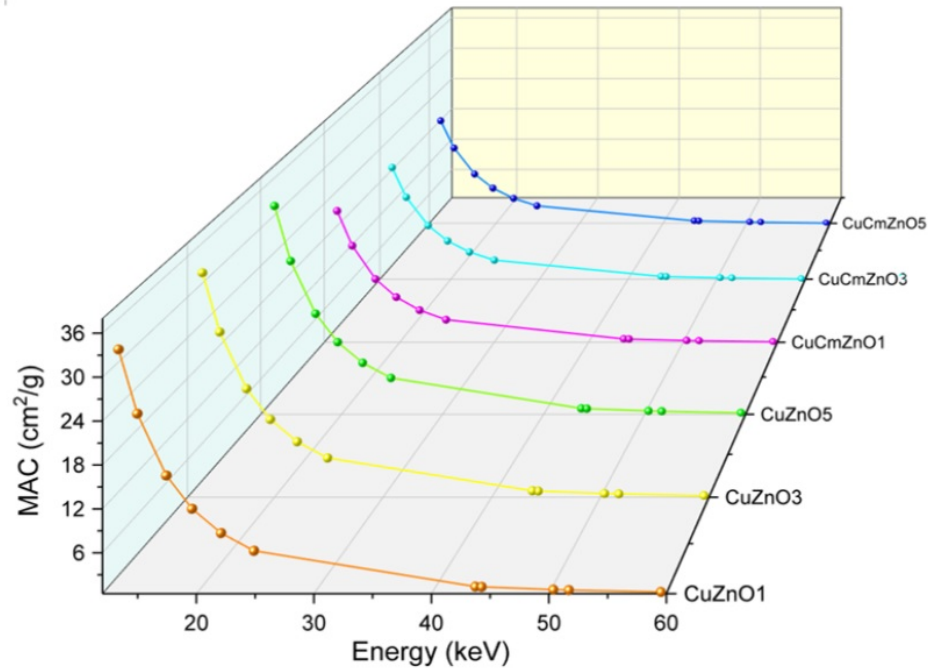

Figure 4.15. MAC values of CZO films.

Table 4.4. Theoretically and experimentally results for MAC of ZCO films of (ZnO, CuZnO1, CuZnO3 and CuZnO5)

Energy (keV)	ZnO		CuZnO1		CuZnO3		CuZnO5	
	Exp.	Theo.	Exp.	Theo.	Exp.	Theo.	Exp.	Theo.
13.37	34.1630± 1.8038	33.8976	34.1561± 1.7078	33.8766	34.1421± 1.1954	33.8234	34.1274± 0.9119	33.7274
14.97	25.3237± 1.3370	24.6787	25.3178± 1.2658	24.2987	25.3059± 0.8861	24.0568	25.2933± 0.6759	23.8933
17.44	16.7858± 0.8862	16.7566	16.7818± 0.8390	16.5456	16.7737± 0.5873	16.2788	16.7651± 0.4480	15.9651
19.63	12.1971± 0.6440	11.9768	12.1938± 0.6096	11.8224	12.1871± 0.4267	11.7787	12.1801± 0.3255	11.9801
22.1	8.8275± 0.4660	8.7345	8.8251± 0.4412	8.5657	8.8203± 0.3088	8.3779	8.8153± 0.2356	8.3153
24.9	6.3782± 0.3367	5.9989	6.3764± 0.3188	5.9946	6.3726± 0.2231	5.9930	6.3687± 0.17025	6.0687
43.74	1.4162± 0.0747	1.4013	1.4158± 0.0707	1.3978	1.4148± 0.0495	1.3798	1.4139± 0.0378	1.3539
44.28	1.3728± 0.0724	1.3757	1.3723± 0.0686	1.3546	1.3714± 0.0480	1.3179	1.3705± 0.0366	1.3005
50.38	0.9952± 0.0525	0.9989	0.9949± 0.0497	0.9945	0.9943± 0.0348	0.9915	0.9937± 0.0265	0.9887
51.7	0.9353± 0.0493	0.9364	0.9350± 0.0467	0.9322	0.9344± 0.0327	0.9312	0.9338± 0.0249	0.9288
59.54	0.6743± 0.0356	0.6657	0.6741± 0.0337	0.6632	0.6737± 0.02359	0.6606	0.6732± 0.0181	0.6532

Table 4.5. Theoretically and experimentally results for MAC of ZCO films of (CuCmZnO1, CuCmZnO3 and CuCmZnO5)

Energy (keV)	ZnO Exp.	ZnO Theo.	CuZnO1 Exp.	CuZnO1 Theo.	CuZnO3 Exp.	CuZnO3 Theo.	CuZnO5 Exp.	CuZnO5 Theo.
13.37	34.1630± 1.8038	33.8976	34.1561± 1.7078	33.8766	34.1421± 1.1954	33.8234	34.1274± 0.9119	33.7274
14.97	25.3237± 1.3370	24.6787	25.3178± 1.2658	24.2987	25.3059± 0.8861	24.0568	25.2933± 0.6759	23.8933
17.44	16.7858± 0.8862	16.7566	16.7818± 0.8390	16.5456	16.7737± 0.5873	16.2788	16.7651± 0.4480	15.9651
19.63	12.1971± 0.6440	11.9768	12.1938± 0.6096	11.8224	12.1871± 0.4267	11.7787	12.1801± 0.3255	11.9801
22.1	8.8275± 0.4660	8.7345	8.8251± 0.4412	8.5657	8.8203± 0.3088	8.3779	8.8153± 0.2356	8.3153
24.9	6.3782± 0.3367	5.9989	6.3764± 0.3188	5.9946	6.3726± 0.2231	5.9930	6.3687± 0.17025	6.0687
43.74	1.4162± 0.0747	1.4013	1.4158± 0.0707	1.3978	1.4148± 0.0495	1.3798	1.4139± 0.0378	1.3539
44.28	1.3728± 0.0724	1.3757	1.3723± 0.0686	1.3546	1.3714± 0.0480	1.3179	1.3705± 0.0366	1.3005
50.38	0.9952± 0.0525	0.9989	0.9949± 0.0497	0.9945	0.9943± 0.0348	0.9915	0.9937± 0.0265	0.9887
51.7	0.9353± 0.0493	0.9364	0.9350± 0.0467	0.9322	0.9344± 0.0327	0.9312	0.9338± 0.0249	0.9288
59.54	0.6743± 0.0356	0.6657	0.6741± 0.0337	0.6632	0.6737± 0.02359	0.6606	0.6732± 0.0181	0.6532

These coefficients are essential in quantifying the attenuation behavior of X-ray and gamma-ray photons as they traverse a medium, with both parameters intrinsically dependent on the photon energy and the elemental composition of the attenuating material. A general decrease in both LAC and MAC values was observed as photon energy increased, consistent with well-established attenuation theory. Absorption of photon energies near or below the electron rest mass is mostly done by the photoelectric effect, giving small thickening attributes a high LAC and MAC that fall roughly as a power of energy, like E 3 or E 4. Low Z materials are very good at absorbing low energy photons. As the energy climbs towards the middle range, the picture changes, with Compton scattering taking the lead but the MAC falling more slowly. Above the energy level of pair production, 1.022 MeV, a clear change takes place, and the MAC may go up higher especially in high Z materials.

As seen in Table .4.5, the addition of copper and copper based The data you

have shown indicate that the extra parts added to the films of ZnO thin make it use less light when light hits. The significant change is that many extra parts make the film weaker at using light when the extra parts grow high and low. These results provide proof of what was found before when Cu covers the top and in the main part of ZnO the film uses less light, and the dots show more because they bounce lighter off the surface. The less light the film uses is likely due to problems and the grain type, which gives back lighter than they get in, and this is more so when the extra parts grow higher in the main part. The MAC for CuZnO samples is greater than for CuCmZnO samples, so CuZnO samples block more light even if they do not have the extra parts. When looking at samples with different levels of doping, it appears that CuZnO thin films are less affected than those with copper extra parts, so they are harder to in terms of change by the dopers how they look and how they work. When films are made to stop rays with high energy, the MFP and Hto VL must be noted. Both are most likely to get larger as the rays get more energy, which means the films are better at blocking the rays with these higher energies and offer safe protection. Figures 4.8. and 4.9. show that the MFP and HVL grow larger as the rays gain more energy; through his is because the mechanism that keeps more rays the photoelectric effect is weaker at higher energies, so fewer rays hit the films and stop. For example, at 51.7 keV, the MFP for normal CuZnO1, CuZnO3, and CuZnO5 was 0.4532 cm, 0.3653 cm, and 0.3357 cm, respectively. The MFP for the complexes CuCmZnO1, CuCmZnO3, and CuCmZnO5 were 0.5547 cm, 0.5557 cm, and 0.5665 cm, respectively. The larger MFP for the complexes shows they are less effective at blocking photons, which makes them less suitable for stopping gamma rays at this energy. At 59.54 keV, the HVL for normal CuZnO1, CuZnO3, and CuZnO5 was 0.4357 cm, 0.3512 cm, and 0.3228 cm, respectively. The HVL for complex CuCmZnO1, CuCmZnO3, and CuCmZnO5 was 0.5328 cm, 0.5329 cm, and 0.5422 cm, respectively. The larger numbers for these copper complex doping negatively impacts on the gamma attenuation performance of ZnO-based thin films at this energy level is supported by the significant rise in HVL, which suggests a decrease in the shielding efficiency of the CuCmZnO samples.

From what we found, CuZnO5 and CuCmZnO1 can stop lighter than the other samples, showing that these materials could do a better job protecting against gamma rays.

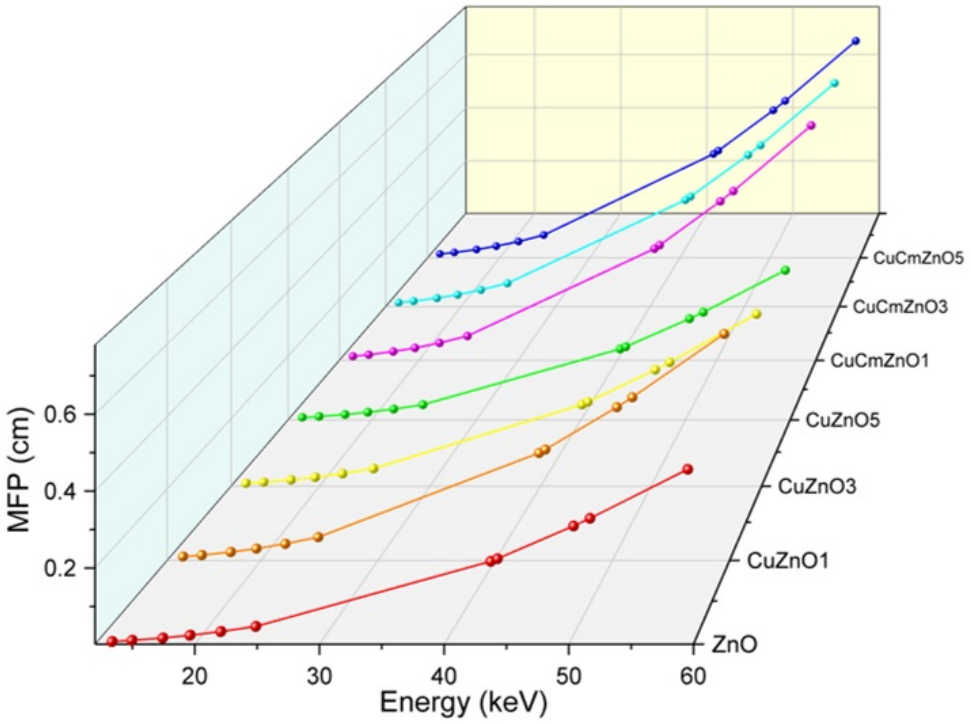

Figure 4.16. MFP values of CZO films.

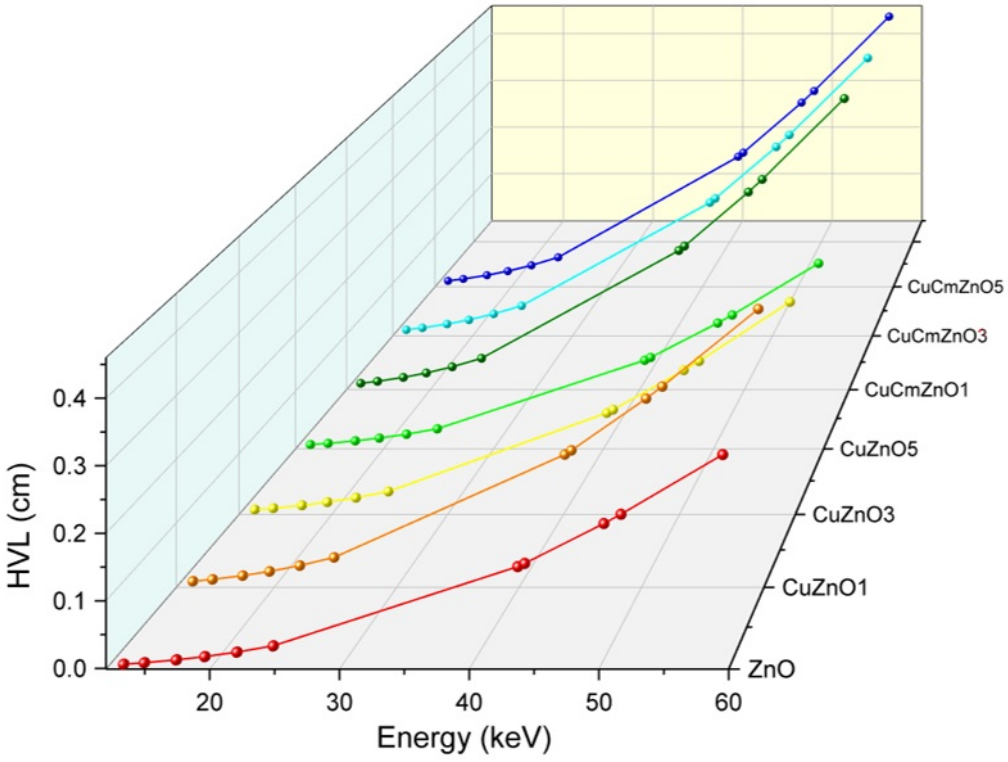

Figure 4.17. HVL values of CZO films.

The effective atomic number Zeff is key to understanding how gamma rays pass through mixtures, just like the atomic number Z does for pure substances. It

gives a clear look at how likely photons are to interact in different systems, especially in materials with many elements, each with their own atomic number. As with the mass attenuation coefficient MAC, Zeff is influenced by the main ways photons interact, such as the photoelectric effect, Compton scatter, and pair production, each of which changes at different energy levels.

In the low energy range (less than 100 keV), the photon count drop is mainly from the photoelectric effect, making MAC and Zeff closely linked. Often this link follows a power-law form, from Zeff to the fourth power to Zeff to the fifth power. Because of this, even small rises in Zeff can greatly increase attenuation. In the middle energy range (100 to 1000 keV), Compton scatter becomes more important, and MAC's relationship to Zeff lessens since Compton scatter depends more on the number of electrons than on atomic number. Still, at high energy (above 1.022 MeV), where pair production dominates, MAC again shows a link roughly to Zeff squared. This makes Zeff a vital tool for studying and comparing how gamma rays pass through various complex materials, especially across different energy levels.

To test the photon interaction behavior of CZO thin films at 13.37 keV, the effective atomic number Zeff was calculated. The Zeff values for both non-doped and copper-doped ZnO samples, like ZnO, CuZnO1, CuZnO3, and CuZnO5, were found to be 26.5073, 26.5013, 26.48916, and 26.4763. For ZnO and the copper-doped ZnO samples called CuCmZnO1, CuCmZnO3, and CuCmZnO5, the Zeff measured 26.5073, 26.4597, 26.3657, and 26.2610. These results reveal a consistent decrease in Zeff with increasing dopant concentration in both doping strategies as seen from Fig. 4.11. However, the decline is more pronounced in the copper-based complexes doped series, indicating a stronger modification of the effective atomic structure due to complexation. Given the strong dependence of photon attenuation (particularly via the photoelectric effect) on Zeff at low photon energies, these reductions in Zeff are expected to negatively influence the gamma-ray absorption capacity of the doped films, especially in the low-energy regime.

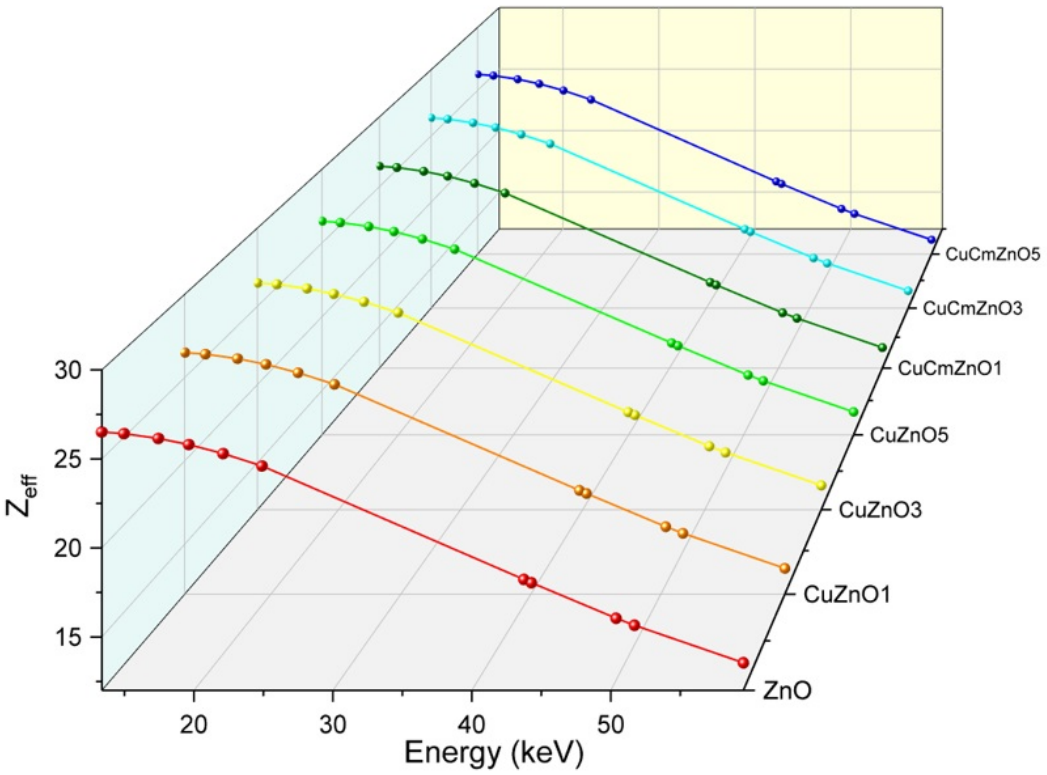

Figure 4.18. Zeff values of CZO films.

4.5.2. Determination of Albedo Parameters

The albedo parameters, which quantifies the fraction of incident photons reflected by a material, is an important metric for evaluating radiation-matter interaction, especially in terms of Compton scattering. Since theoretical models are insufficient for predicting reflectivity behavior, experimental determination of photon reflection parameters is essential.

Figs. 4.14-4.16 demonstrate how the albedo number (AN), albedo energy (AE), and albedo dose (AD) vary sample thickness and concentration (Table 4.6) at a 180° scattering angle. Zeff values computed using the EpiXS software in photon energy of 59.54 keV are very close to each other. Accordingly, the correlation between albedo parameters and Zeff was not examined in this study due to the negligible differences in effective atomic number (13.5505, 13.55138, 13.55312, 13.55497, 13.4676, 13.30774, 13.13503 for ZnO,

CuZnO1, CuZnO3, CuZnO5, CuCmZnO1, CuCmZnO3, CuCmZnO5, respectively). As seen from Figs. 4.14-4.16, the copper-based complexes (CuCmZnO1, CuCmZnO3, CuCmZnO5) demonstrated the strongest correlation

between compositional concentration and albedo parameters variation. Among all CZO thin films investigated, the CuCmZnO5 sample exhibited the highest values of AN, AE, and AD, indicating superior reflectance and minimal photon absorption. The pure ZnO exhibits a heterogeneous surface, which promotes photon reflection. In contrast, CuZnO5 and CuCmZnO5 display more homogeneous surface, resulting in reduced absorption and increased reflectivity.

The fabricated thin films demonstrate potential for use as anti-reflective coatings in high-tech fields such as nuclear engineering, space technology, and medical instrumentation. For example, in medical applications: X-and gamma rays hitting the floor or ceiling of a treatment room can be backscattered toward the patient. Measured albedo coefficients for various materials are crucial for estimating scattered radiation doses and for maintaining patient and personnel safety. Improves dose planning accuracy in radiation therapy. Also, it reduces risk of unintended exposure from secondary radiation.

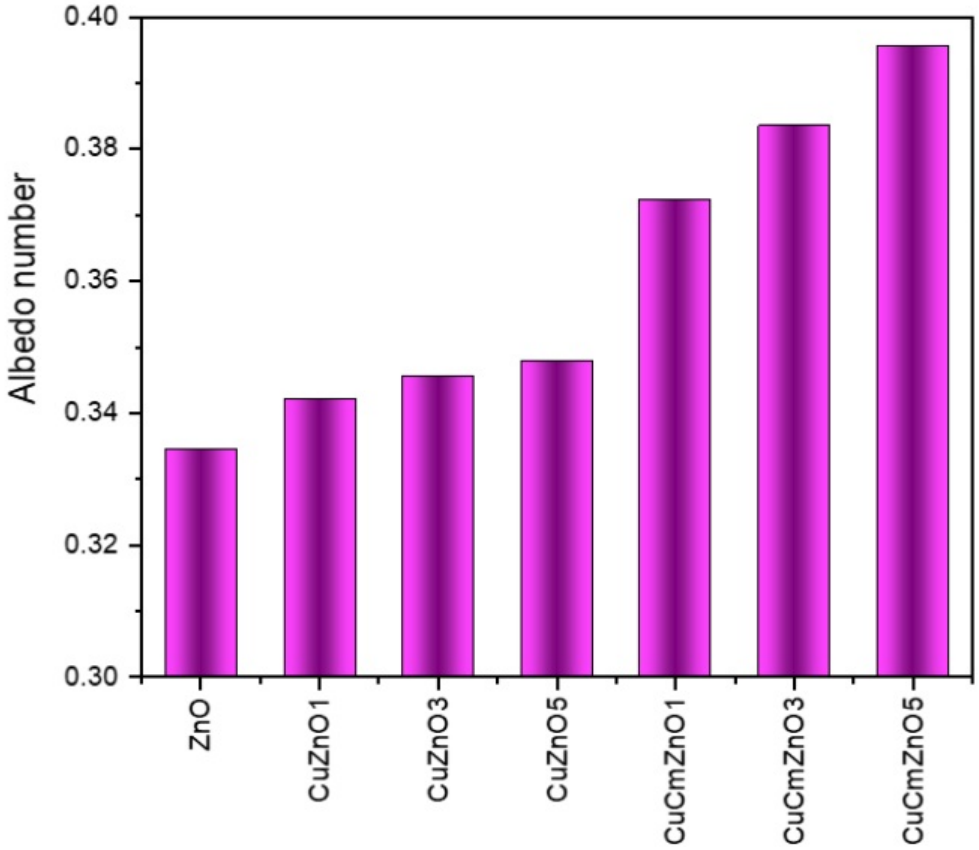

Figure 4.19. Albedo numbers of CZO thin films.

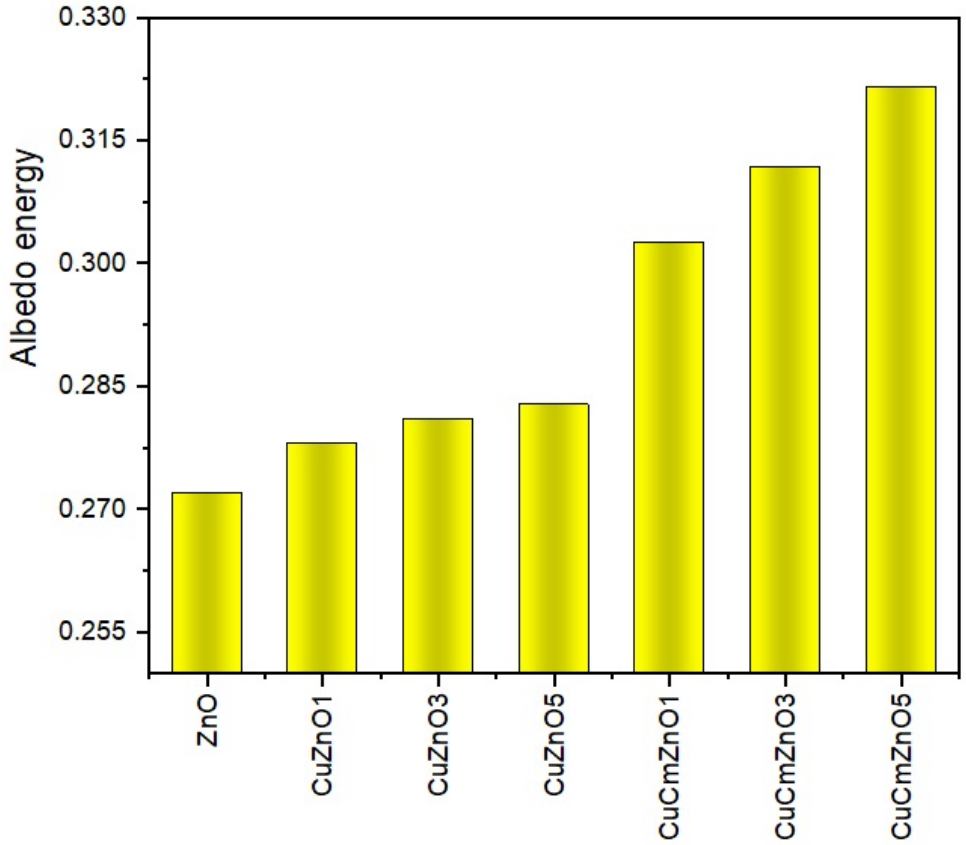

Figure 4.33. Albedo energies of CZO thin films.

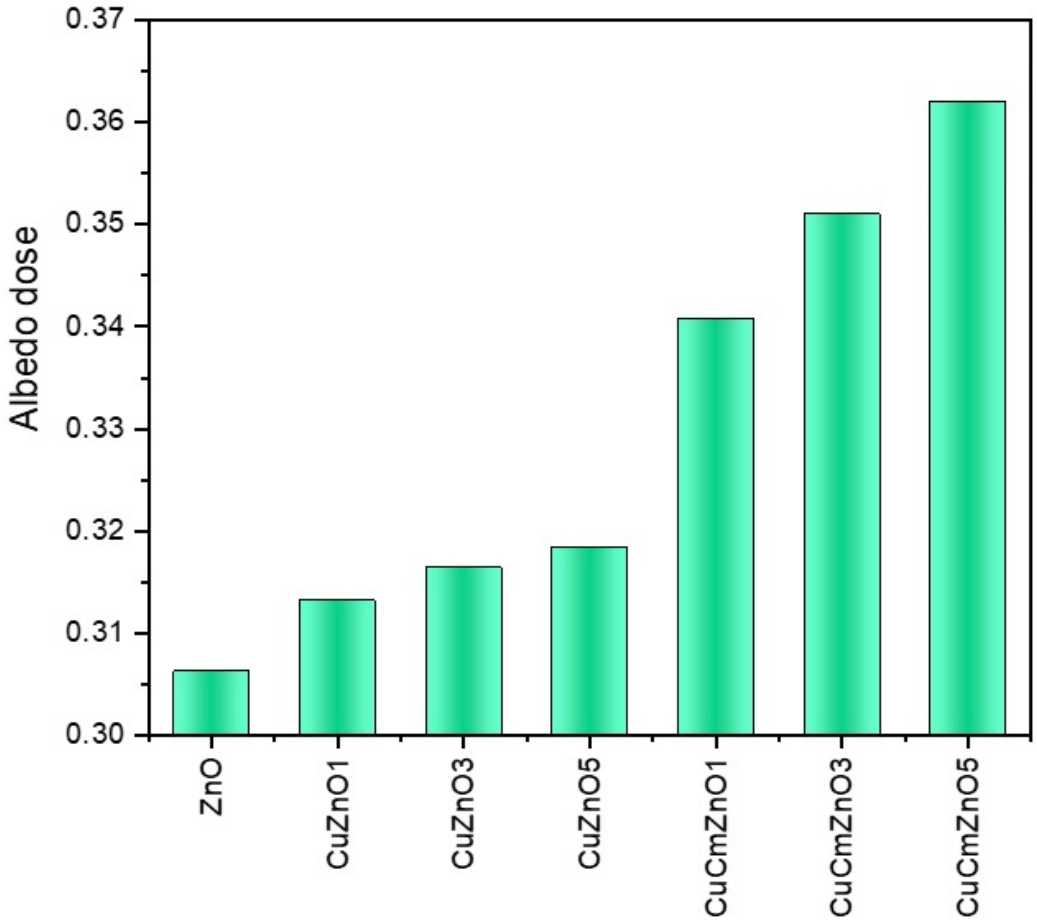

Figure 4.34. Albedo doses of CZO thin films.

4.5.3. Neutron Attenuation

The neutron equivalent dose rates for CZO composite films were experimentally evaluated. The background dose rate was measured as 1.2039 μSv/h. To enhance the reliability of the data, repeated measurements were conducted, and statistically anomalous values were excluded due to the inherently stochastic nature of nuclear interactions and detector behavior. The absorbed neutron equivalent dose rates (μSv/h) were recorded for all samples. As illustrated in Fig. 4.17, among the investigated films, the CuCmZnO5 demonstrated the most effective neutron attenuation performance. The CuCmZnO5 sample absorbed 21.82 of the doses emitted from fast neutron source. When 5 copper-based complexes were added, neutron absorption increased by approximately 15, indicating that copper complex's presence has a positive effect on the overall neutron attenuation performance of the material. The neutron shielding properties of CZO films are shown in Table 4.6.

Table 4.6. The neutron shielding parameters of CZO films.

The thermal neutron attenuation parameters of CZO films (25.4 meV)							
Parameter	ZnO	CuZnO1	CuZnO3	CuZnO5	CuCmZnO1	CuCmZnO3	CuCmZnO5
Σ (cm^{-1})	0.0285	4.9377	5.9379	6.3962	3.304	3.1779	3.14755
MFP (cm)	35.0877	0.2025	0.1684	0.15634	0.30266	0.31467	0.31771
HVL (cm)	24.3157	0.1403	0.1167	0.1083	0.20975	0.21807	0.22017
The fast neutron attenuation parameters of CZO films (4 MeV)							
Parameter	ZnO	CuZnO1	CuZnO3	CuZnO5	CuCmZnO1	CuCmZnO3	CuCmZnO5
Σ (cm^{-1})	0.01874	4.9007	5.8866	6.3383	3.26491	3.13503	3.10374
MFP (cm)	53.3617	0.2040	0.1698	0.1577	0.30629	0.31898	0.32219
HVL (cm)	36.9797	0.1414	0.1177	0.1093	0.21226	0.22105	0.22328
The fast neutron removal attenuation parameters of CZO films							
Parameter	ZnO	CuZnO1	CuZnO3	CuZnO5	CuCmZnO1	CuCmZnO3	CuCmZnO5
Σ (cm^{-1})	0.07359	0.1417	0.1735	0.1881	0.11804	0.12006	0.12057
MFP (cm)	13.588	7.0538	5.7607	5.3155	8.4717	8.3291	8.29407
HVL (cm)	9.4170	4.8883	3.9921	3.6837	5.87089	5.77207	5.74779
Gamma-Ray attenuation parameters of CZO films (59.54 keV)							
Parameter	ZnO	CuZnO1	CuZnO3	CuZnO5	CuCmZnO1	CuCmZnO3	CuCmZnO5
μ (cm^{-1})	2.1894	2.1894	2.1894	2.1894	2.1894	2.1894	2.1894
MFP (cm)	0.4567	0.6286	0.5066	0.4656	0.7686	0.7688	0.7821
HVL (cm)	0.3165	0.4356	0.3511	0.3226	0.5326	0.5327	0.5420

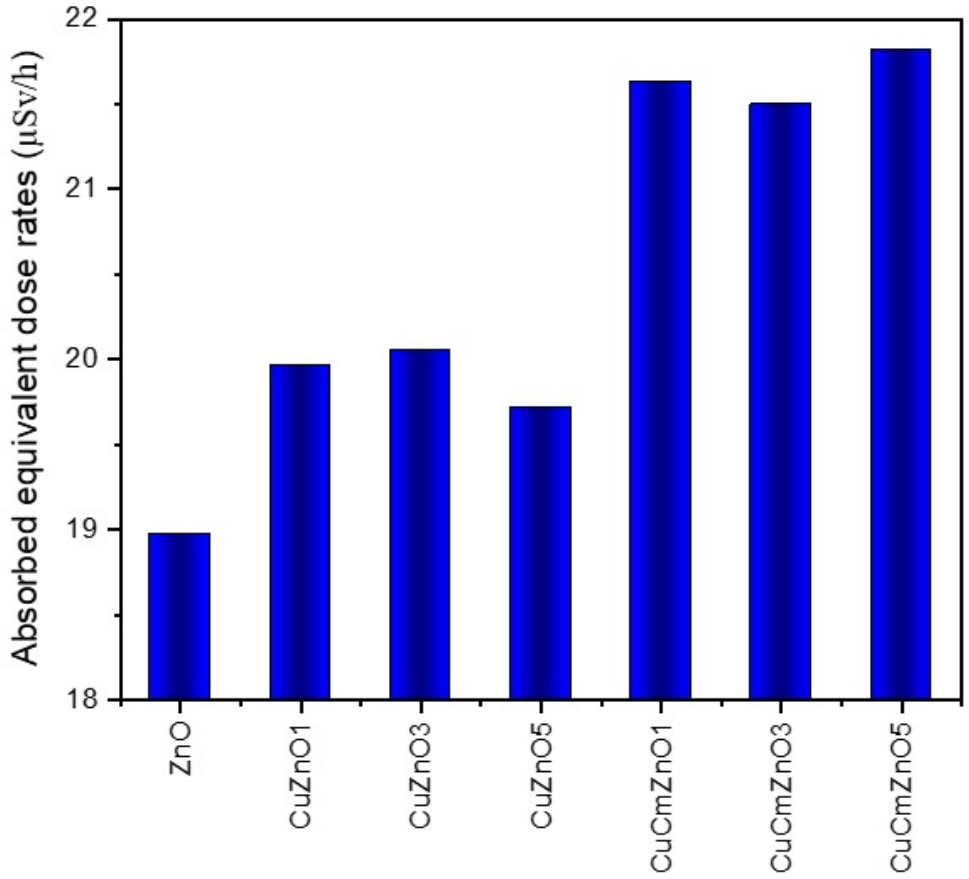

Figure 4.35. Neutron absorbed equivalent dodse rates fo CZO films.

Table 4.6 shows CZO thin film with a thickness of 0.031 to 0.037 cm can block some thermal and fast neutrons. Its blocking speed is high when fast neutrons are more energetic, and their effect on living things is still high, measured in units called µSv/sec.

The cross-section for fast neutrons is a key nuclear factor showing how good a material is at soaking up high-energy neutrons, usually above 1 MeV energy. Because these neutrons are fast and have high energy, they are very effective in causing damage or other effects, so shield materials must be designed especially for them. If the section is in barns, 1 barn being 10.24 cm², it depends on the material's nuclear makeup and what it is made of. Materials with atoms of a high number or those with isotopes that trap neutrons, like cadmium, boron, and certain rare earths, are much better for soaking up fast neutrons. It is useful to find the fast neutron cross-section to see how well CZO thin film can be used in reactor shields.

ZnO is not a strong material for soaking up neutrons, but when copper is added, it can attract neutrons. This is very useful in places with high radiation, like nuclear reactors, or in medical clinics for treatments, or space stations, where neutrons can go through buildings and materials easily, making it necessary to prevent them and keep the structure strong and safe. Lastly, a material that can soak up neutrons faster is better at blocking them, so its overall use is better in shield systems.

5. DISCUSSION

The studied Cu doped ZnO grown by sol-gel spin coating process has contributed significant understanding of the physical and optical effects and radiation behavior of the material when copper atoms are integrated into the matrix. Structurally, X-ray diffraction (XRD) patterns usually affirm the polycrystalline nature of ZnO in the hexagonal quartzite form, agreeing with earlier literature (Özgür et al., 2005). The entry of Cu ions into the ZnO crystal lattice influences crystallinity and grain size and in many cases leads to a partial reduction of height depth as well as a minimal change in diffraction angles. This adjustment is caused due to the substitution of Zn^{2+} ions (ionic radius ~0. seventy-four Å) by the assistance of Cu^{2+} ions (ionic radius ~0. seventy-three Å), resulting in lattice distortion and stress in the crystal framework (Thakur et all., 2014). Stress and defects provided by incorporating doping are primarily responsible for modulating the digital and optical properties of the films.

Optically, UV-Vis spectroscopy shows that Cu doping causes a decrease within the optical band hole compared to undoped ZnO films. Such narrowing of band holes, which is encountered as a redshift within the absorption edge, is typically described with the assistance of the introduction of extra power stages within band shape owing to Cu-related disorder states and increased sp-d trade interactions between the localized d-electrons of copper and ZnO's band electrons (Look et all, 2001; Pearton et al., 2005). Lower in band hole is useful for packages like photovoltaics and photo catalysis in which noted mild absorption is required. Besides, the growth in Cu awareness can lead to improved sub-band hole absorption, that is, the beginning of intra-hole states and capacity provider recombination centers. Such things change how good the thin film is at letting and bouncing light on it they can make a big change in how good onto electronic parts are.

For the subject of how it reacts to light, people can know for sure that Cu-ZnO thin films change how they react to ionizing light like gamma rays or X rays in ways that depend on doping. Putting copper into ZnO makes the thin film stand up better to light by giving it spots where parts made by light can come together, lowering the chance that the light will cause lasting faults that lower the quality of the material (Kumar et all., 2019). When light hits, it usually causes more faults to appear, including missing oxygen parts and extra zinc parts, which can make the thin film shift how it’s made and how it reacts to light, like how bright it glows when light hits it and how deep the glow goes. Studies show that Cu-ZnO thin films made

by the sol-gel process have a mixed bag of faults that form and go away with light, and the amount of copper added is an important part of how this all works. This makes Cu-ZnO a good choice of parts that must work in places with lots of light or radiation.

To sum up, the sol-gel spin coating method is good to make Cu-doped ZnO thin films better and give them traits you can order to make them work better. Putting copper in makes the lattice change a lot and how electrons move in it, making the band structure different and how faults come and go, which all change how well the thin film works. These facts fit with recent studies and ideas in the research (Singh et al., 2018; Zhang et al., 2023) and show how Cu-ZnO thin films can be used in parts that have to be light-sensitive, find light, or stay safe in places with lots of radiation. For later work, people should try to make the doping levels and heat treats after the films are made better to get more control over how they work for different jobs.

6. CONCLUSION

The structural, optical, and radiation effects on Cu doped ZnO thin films formed by sol gel spin coating method are studied in this work. Seven samples were examined: undoped ZnO, Cu doped at various levels, and ZnO doped with Cu complexes. XRD analysis, UV Vis, and Raman spectroscopy subjected to radiation were used to assess crystallinity, optical properties, and lattice stability, respectively.

XRD characterization confirmed that all the film compositions retained hexagonal wurtzite structure with varied intensity and broadening of some peaks with introduction of Cu and Cu-complex. The crystallite decreases were even more conspicuous with higher Cu doping concentrations, indicating lattice strain and defect formation. The structural aberrations were further enhanced upon irradiation, especially in complex-doped films, with poorer ionizing radiation resistance.

UV-Vis spectroscopy further showed Cu doping to lower the band gap, especially for 3% and 5% doping levels that would be understandable because of localized state appearance within the band structure. Increased visible range absorption further showed photovoltaic applications in combination with TCO device applications. Cu-complex-containing films, however, further showed lowered transmittance as well as anomalous absorption features, which can be explained by inhomogeneous doping as well as structural instability.

Raman spectra confirmed the radiation-induced degradation of the vibrational modes, especially in Cu-complex films. ZnO high-energy peak E_2 (high) at ~438 cm^{-1} significantly decreased in intensity and was broadened with high radiation dose and Cu doping. It confirms the generation of oxygen vacancies, zinc interstitials, and other radiation-produced defects. Cu-doped ZnO (1%–3%) exhibited relatively better structural stability in comparison to Cu-complex counterparts.

7. RECOMMENDATIONS

Cu doping of ZnO thin films via sol-gel spin coating was shown to be a promising method for modifying structural and optical parameters. The study justifies the use of Cu-ZnO thin films in photovoltaic, sensor, and transparent electronics devices. The type and amount of doping must be optimized to some extent, particularly in radiation-exposed applications. Further work would focus on radiation hardening and on enhancing doping profile uniformity to provide more stable devices over the long term with such films.

REFERENCES

Abraham, P., Shaji, S., Avellaneda, D. A., Aguilar-Martínez, J. A., & Krishnan, B. (2023). Sb2S3 thin films: From first principles to in situ crystalline thin film growth by ultrasonic spray pyrolysis. Materials Science in Semiconductor Processing, 156, 107269.

Amani, F., Bidadi, H., & Mohammadi, M. A. (2024). Structural and optical studies of copper doped zinc oxide thin films synthesized by co-precipitation method. Optical Materials, 156, 115965.

Arunodaya, J., Nayak, N., & Sahoo, T. (2023). Tailoring the optical and electrical behavior of Cu2O/ZnO heterojunction by varying the Zn2+ ion concentration for solar-cell applications. Micro and Nanostructures, 174, 207488.

Bai, J., Li, J. S., Wang, J., Cui, J., Li, L. Y., Kou, H. C., & Liaw, P. K. (2015). Strain-rate-dependent deformation behavior in a Ti-based bulk metallic glass composite upon dynamic deformation. Journal of Alloys and Compounds, 639, 131-138.

Buzok, E. B., Yalcin, S., Demircan, G., Yılmaz, D., Aktas, B., & Aytar, E. (2024). The structural, optical, electrical and radiation shielding properties of Co-doped ZnO thin films. Radiation Physics and Chemistry, 222, 111840.

Buzok, E. B., Yalcin, S., Demircan, G., Yılmaz, D., Aktaş, B., & Aytar, E. (2025). Effect of a Cobalt Complex on the Structural, Optical, Electrical, and Anti-Reflective Properties of ZnO Thin Films. Ceramics International.

Caglar, M., & Yakuphanoglu, F. (2012). Structural and optical properties of copper-doped ZnO films derived by sol–gel. Applied Surface Science, 258(7), 3039–3044.

Chander Joshi, B., & Chaudhri, A. K. (2022). Sol–gel-derived Cu-doped ZnO thin films for optoelectronic applications. ACS omega, 7(25), 21877-21881.

Chen, C., Wei, Y., Chen, D., & Jiao, X. (2011). Indium oxide nanocrystals: capping-agent-free synthesis, size-control mechanism, and high gas-sensing performance. Materials Chemistry and Physics, 125(1-2), 299-304.

Chen, G. J., Jian, S. R., & Juang, J. Y. (2018). Surface analysis and optical properties of Cu-doped ZnO thin films deposited by radio frequency magnetron sputtering. Coatings, 8(8), 266.

Demircan, G., Acikgoz, A., Yalcin, S., Aytar, E., Balak, M. V., & Aktas, B. (2023). The influence of doping perimidine ruthenium complexes on structural, optic, and residual stress properties of ZnO thin films. Brazilian Journal of Physics, 53(1), 20.

Demircan, G., Gurses, E. F., Acikgoz, A., Yalcin, S., & Aktas, B. (2020). Effects of spin coating parameters on stress, electrical and optical properties of multilayer ZnO thin film prepared by sol–gel. Molecular crystals and liquid crystals, 709(1), 61-69.

Demircan, G., Gurses, E. F., Aktas, B., Yalcin, S., Acikgoz, A., Ceyhan, G., &

Balak, M. V. (2023). Sol–gel synthesis of Si-ZnO, Ti-ZnO and Si-Ti-ZnO thin films: impact of Si and Ti content on structural and optical properties. Materials Today Communications, 34, 105234.

Demircan, G., Yalcin, S., Alivi, K., Ceyhan, G., Acikgoz, A., Balak, M. V., ... & Das, R. (2022). The effect of Co and Mn Co-Doping on structural and optical properties of ZnO thin films. Optical Materials, 126, 112163.

Du, X., Zhang, W., Zhang, M., Ji, Y., Su, K., & Li, Z. (2022). Dual-Metal Zeolitic Imidazolate Framework Derived Highly Ordered Hierarchical Nanoarrays on Self-Supported Carbon Fiber for Oxygen Evolution. Materials, 15(12), 4170.

Hamel, M., Trocmé, M., Rousseau, A., & Darbon, S. (2017). Red-emitting liquid and plastic scintillators with nanosecond time response. Journal of Luminescence, 190, 511-517.

Ivanova, T. & Harizanova, A. (2025). The effect of substrate type on the optical and structural properties of sol–gel ZnO and ZnO:Ga films. Molecules, 30(16), 3342.

Jabarov, S. H., Aliyeva, V. B., Mammadov, T. G., Mammadov, A. I., Kichanov, S. E., Dubrovinsky, L. S., ... & Dang, N. T. (2018). High pressure Raman study of layered semiconductor TlGaSe2. Materials Science-Poland, 36(2), 203-208.

Jagadish, K. A., & Kekuda, D. (2024). Thermal annealing effect on phase evolution, physical properties of DC sputtered copper oxide thin films and transport behavior of ITO/CuO/Al Schottky diodes. Applied Physics A, 130(5), 315.

Kayani, Z. N., Iram, S., Rafi, R., Riaz, S., & Naseem, S. (2018). Effect of Cu doping on the structural, magnetic and optical properties of ZnO thin films. Applied Physics A, 124(7), 468.

Kumar, S., Ahmed, F., Ahmad, N., Shaalan, N. M., Kumar, R., Alshoaibi, A., ... & Kumari, K. (2022). Structural, morphological, optical and magnetic studies of Cu-doped ZnO nanostructures. Materials, 15(22), 8184.

Kuriakose, S., Satpati, B., & Mohapatra, S. (2015). Highly efficient photocatalytic degradation of organic dyes by Cu doped ZnO nanostructures. Physical Chemistry Chemical Physics, 17(38), 25172-25181.

Licurgo, J. S. C., & Paes Junior, H. R. (2018, October). Morphological, structural, electrical and optical properties of copper-doped zinc oxide films deposited by spray pyrolysis. In Materials Science Forum (Vol. 930, pp. 79-84). Trans Tech Publications Ltd.

Mattox, D. M. (2010). Handbook of Physical Vapor Deposition (PVD) Processing (2nd ed.). Oxford: William Andrew / Elsevier.

RESUME

PERSONAL INFORMATION

Name Surname	:	KOCHAR SALIH ARIF ARIF
Date of birth	:	0000-00-00
Place of birth	:	IRAK
Telephone	:	0500 000 00 00
E-mail	:	kocharsalih6@gmail.com